

UC Berkeley

UC Berkeley Previously Published Works

Title

Projecting climate change in South America using variable-resolution Community Earth System Model: An application to Chile

Permalink

<https://escholarship.org/uc/item/3gb5s3s7>

Journal

International Journal of Climatology, 42(4)

ISSN

0899-8418

Authors

Bambach, Nicolas E
Rhoades, Alan M
Hatchett, Benjamin J
[et al.](#)

Publication Date

2022-03-30




DOI

10.1002/joc.7379

Peer reviewed

RESEARCH ARTICLE

Projecting climate change in South America using variable-resolution Community Earth System Model: An application to Chile

Nicolas E. Bambach¹  | Alan M. Rhoades²  | Benjamin J. Hatchett³  |
Andrew D. Jones² | Paul A. Ullrich¹ | Colin M. Zarzycki⁴

¹Department of Land, Air, and Water Resources, University of California, Davis, Davis, California, USA

²Climate and Ecosystem Sciences Division, Lawrence Berkeley National Laboratory, Berkeley, California, USA

³Western Regional Climate Center, Desert Research Institute, Reno, Nevada, USA

⁴Department of Meteorology and Atmospheric Science, Pennsylvania State University, University Park, Pennsylvania, USA

Correspondence

Nicolas E. Bambach, University of California, Davis, Davis, CA, USA.
Email: nbambach@ucdavis.edu

Alan M. Rhoades, Climate and Ecosystem Sciences Division, Lawrence Berkeley National Laboratory, Berkeley, California, USA
Email: arhoades@lbl.gov

Funding information

National Science Foundation, Grant/Award Numbers: EF1137306/MIT, 5710003122; United States Department of Energy, Grant/Award Numbers: DE-AC02-05CH11231, DE-SC0016605; Centro de Cambio Global at Pontifical Catholic University of Chile

Abstract

We introduce variable-resolution enabled Community Earth System Model (VR-CESM) results simulating historical and future climate conditions at 28 km over South America and 14 km over the Andes. Three 30-year simulations are performed: a historic (1985–2014), a near future (2030–2059), and an end-century (2070–2099) simulation under the RCP8.5 scenario. Historic results compare favourably to several temperature and precipitation reanalysis products, though local biases are present, particularly during austral summer. Future simulations highlight broad warming patterns (+3–6°C by end-century) and heterogeneous precipitation responses across South America that qualitatively agree with prior modelling efforts. Our results reveal that the interaction between temperature and precipitation changes produce shifts in several Köppen–Geiger climates. Notable changes include the near-elimination of the Andean Tundra or Alpine climates, a 15% decrease in Tropical Rainforests and a Tropical Savannah expansion of 20%. To provide a regionally focused analysis of projected climate change and to illustrate the benefits of variable resolution modelling, we analyse changes in the magnitude and trend in seasonal and daily temperature and precipitation in Chile. We also examined several metrics [e.g., snow water equivalent (SWE), temperatures on wet days, and days below 0°C] to evaluate potential impacts of climate change on the Chilean cryosphere between the end-of-century and historic periods, finding wide-ranging indications of cryospheric decline. These changes are interpreted through reductions in the timing (1–2.5 months earlier peak SWE) and magnitude (200–1,000 mm SWE decreases) of water stored as snow in the Andes, a 10–30% decrease in number of cool season wet days with temperatures below 1°C, and 50–200 fewer days (annually) with minimum temperatures below 0°C. Our aim in producing a high-resolution dataset of climate projections

Nicolas E. Bambach, Alan M. Rhoades, Benjamin J. Hatchett, Andrew D. Jones, Paul A. Ullrich, and Colin M. Zarzycki (all authors) contributed equally to this work.

This is an open access article under the terms of the Creative Commons Attribution-NonCommercial License, which permits use, distribution and reproduction in any medium, provided the original work is properly cited and is not used for commercial purposes.

© 2021 The Authors. *International Journal of Climatology* published by John Wiley & Sons Ltd on behalf of Royal Meteorological Society.

from VR-CESM is to support analyses of climate change throughout South America but especially in vulnerable montane regions and to provide additional results for comparison with previous, ongoing, and upcoming modelling efforts.

KEYWORDS

Andes, Chile, climate change, Earth System Models, hydroclimate, South America, variable-resolution global climate models

1 | INTRODUCTION

The recent Intergovernmental Panel on Climate Change report indicates *medium-to-high confidence* that since the late 20th century, human-induced climate change has increased temperatures and made precipitation patterns more variable and extreme in South America (Field, 2014). The ramifications of these changes are corroborated by studies that investigate enhanced droughts (Garreaud *et al.*, 2017, 2020; Naumann *et al.*, 2019; Rodrigues *et al.*, 2020), more severe fires (Bowman *et al.*, 2019; Fonseca *et al.*, 2019; Gómez-González *et al.*, 2019), more frequent heat waves (Rusticucci *et al.*, 2016; Feron *et al.*, 2019; Gómez-González *et al.*, 2019) and flood events (Bozkurt *et al.*, 2016; Ávila *et al.*, 2019; Rondanelli *et al.*, 2019; Valenzuela and Garreaud, 2019; Huggel *et al.*, 2020; Poveda *et al.*, 2020), and substantial cryospheric decline (Huss *et al.*, 2017; Masiokas *et al.*, 2020). These hazards highlight the need for climate model projections at scales relevant to decision making (Gutowski *et al.*, 2020), particularly since there may not be historical analogues that can be used for climate adaptation. However, a limited number of regional climate model (RCM) experiments have been conducted over South America and only one RCM, the Brazilian National Institute for Space Research Eta model, has been developed within the region (Chou *et al.*, 2000). Solman (2013) identified that over the last two decades, less than 100 model-based studies were published and only a handful of coordinated regional downscaling experiments have been performed over South America. These experiments include: the Coordinated Regional Climate Downscaling Experiment [CORDEX, (Solman *et al.*, 2013; Solman, 2013)], the Europe-South America Network for climate Change Assessment [CLARIS, (Boulanger *et al.*, 2010)] and impact studies in the La Plata Basin [CLARIS LPB, (Penalba *et al.*, 2014)], and, most recently, the Universidad de Chile RegCM4 and Eta RCM simulations for Chile (Bozkurt *et al.*, 2019).

These modelling experiments represent a monumental effort and a major step forward to informing climate change policy throughout South America. However, most

RCM simulations in these experiments were performed at ~ 50 km horizontal resolution with added value from the forcing global climate models shown to be model-dependent (Solman and Blázquez, 2019). Although a best-attempt given limited computational resources, ~ 50 km horizontal resolution is insufficient to resolve the diverse microclimates that arise due to the complexity of South American terrain, especially along the coast and in regions near the extreme topographic gradients resulting from the Andes. Giorgi (2019) notes that substantial added value in model fidelity, particularly in regions of complex terrain, occurs at resolutions of ~ 10 – 15 km. Given this resolution-dependence, it is not surprising that the multi-model ensemble of CORDEX simulations showed considerable biases, even in climatological averages of surface temperature and precipitation. These biases were attributed to several factors such as overly coarse model resolution, land-surface parameterizations, and a lack of RCM development within South American institutions (Solman, 2013).

One of the major features that need to be resolved to increase model performance over South America is the Andean mountains. Extending more than 8,000 km from north to south, the South American Andes are the longest continental mountain range in the world (Espinoza *et al.*, 2020; Masiokas *et al.*, 2020) and the second largest by area (Huss *et al.*, 2017). They extend continuously from the North Pacific Coast of South America ($\sim 10^\circ\text{N}$) to the southernmost tip of the continent in the Patagonian archipelago ($\sim 52^\circ\text{S}$). Seven countries with ~ 90 million people rely on the Andes as a source of water, energy, minerals, timber and agricultural products. The Andes are considered the most biodiverse region in the world and are home to numerous ecosystems, endemic species, and indigenous cultures (Pabón-Caicedo *et al.*, 2020). The northwestern flanks of the Andes are home to one of the wettest regions of the world (mean annual precipitation totals of $\sim 13,000$ mm). In the northern tropical Andes, the eastern flanks provide rainfall ($\sim 7,000$ mm $\cdot\text{year}^{-1}$) that form the birthplace of the Amazon River (Espinoza *et al.*, 2020). In contrast, to the west of the subtropical Andean crest lies the hyperarid

Atacama Desert where a confluence of regional ocean and atmospheric circulations and the blocking effects of topography result in annual precipitation totals as low as $\sim 5 \text{ mm}\cdot\text{year}^{-1}$ (Garreaud *et al.*, 2010).

Studies evaluating regional climate change along the Andes are needed due to the critically important ecosystem services they provide and their vulnerability to climatic change (Masiokas *et al.*, 2020). A meta-analysis by Huss *et al.* (2017) indicates that several Andean regions are heavily reliant (50% in some regions) on water derived from snow and glacial melt. These areas could face upwards of an 80% reduction in glacier volume by end-century, with some studies indicating Andean glaciers are among the fastest shrinking on Earth (Dussaillant *et al.*, 2018). Elevation-dependent warming has not been systematically observed in the Andes (Pabón-Caicedo *et al.*, 2020). This lack of observation could be partly due to the sparse network of Andean mountain observations in both space and time (Viviroli *et al.*, 2011; Ochoa-Tocachi *et al.*, 2018; Condom *et al.*, 2020), as well as the influence of interdecadal climate variability (Vuille *et al.*, 2015). However, projected warming may trigger accelerated snow and ice loss due to snow-albedo feedbacks (Pepin *et al.*, 2015).

Many South American countries are embodied by the Andes in some fashion. The Andes form nearly the entire western border of Chile, $\sim 4,500 \text{ km}$, and nearly 64% of Chile's territories are mountains (FAO, 2012). Thus, Chile heavily relies on natural services provided by its mountain areas for some of the most arid and wettest parts of the Andes. Currently, Chile is experiencing one of the most severe droughts on record (Garreaud *et al.*, 2020). Yet during this same period, several extreme precipitation events have affected both densely populated and rural areas throughout the country (Bozkurt *et al.*, 2016; Rondanelli *et al.*, 2019; Valenzuela and Garreaud, 2019). Moreover, extreme high temperatures and heatwaves are becoming more frequent and harmful along the foothills of Chile and have set the stage for severe wildfires (Gómez-González *et al.*, 2019).

Providing a quantitative, physically based, and decision-relevant estimate of anthropogenic climate change requires the use of high-resolution climate models (Gutowski *et al.*, 2020). We introduce model results from a set of historical and future climate simulations of South America using the variable-resolution enabled Community Earth System Model (VR-CESM) at 28 km over all of South America and 14 km over the Andes, hereafter referred to as VR-Andes for this specific study. Three 30-year simulations were performed: a historic (1985–2014), a near future (2030–2059), and an end-century (2070–2099) under Representative Concentration

Pathway 8.5 (RCP8.5) scenario. VR-Andes is a novel, regional telescoping approach that allows for high-resolution Earth System Model (ESM) simulations at considerably less computational cost than conventional ESMs (Skamarock *et al.*, 2012; Harris and Lin, 2013; Rauscher and Ringler, 2014; Zarzycki *et al.*, 2014b, 2015; Ferguson *et al.*, 2016).

These simulations provide a more consistent global-to-regional downscaling approach than conventional RCMs whereby large-scale dynamics, atmosphere–ocean teleconnections and cross-scale interactions are simulated within a single ESM simulation. The use of a single ESM also eliminates the multi-model cascade of bias associated with conventional RCMs and ESMs, which also demonstrate a weak “home-field advantage” in performance based on the country where they were developed (Watterson *et al.*, 2014). The variable resolution grid used in this study is illustrated in Figure 1, which shows the regional telescoping performed in this study with a base 111 km global horizontal resolution that is refined to 55 km over the east Pacific, 28 km over the entire South American continent and, finally, to 14 km over the South American Andes.

Further, the fidelity of VR-CESM simulations have been extensively evaluated over the last half-decade, especially in the representation of the processes that shape Atlantic and Pacific tropical and extra-tropical cyclones (Zarzycki and Jablonowski, 2014; Zarzycki *et al.*, 2014a; Zarzycki *et al.*, 2015, 2016; Zarzycki, 2016) and, of relevance to this study, the mountainous western United States (Huang *et al.*, 2016; Huang and Ullrich, 2016; Rhoades *et al.*, 2016; Huang and Ullrich, 2017; Rhoades *et al.*, 2017; Wu *et al.*, 2017; Gettelman *et al.*, 2018; Rhoades *et al.*, 2018; Wang *et al.*, 2018; Wang and Ullrich, 2018; Xu *et al.*, 2018; Rhoades *et al.*, 2020a, 2020b) showing comparable performance to widely used RCM approaches. While telescoping ESMs such as VR-Andes add value to modeling studies and provide improvements over RCMs, they are not without problems. These problems arise due to a lack of development of scale-aware physics parameterizations (e.g., convection, entrainment, turbulence, and cloud macrophysics) and the use of the hydrostatic approximation in the dynamical core at sub-10 km resolutions (Arakawa and Jung, 2011; Herrington and Reed, 2017, 2020).

We begin with details regarding model set-up, datasets used, and data analysis approaches (Section 2). Then we evaluate the veracity of the VR-Andes downscaling approach over South America against several observation-based temperature and precipitation reanalysis products (Section 3.1). We next assess projected near-future and end-century changes in seasonal

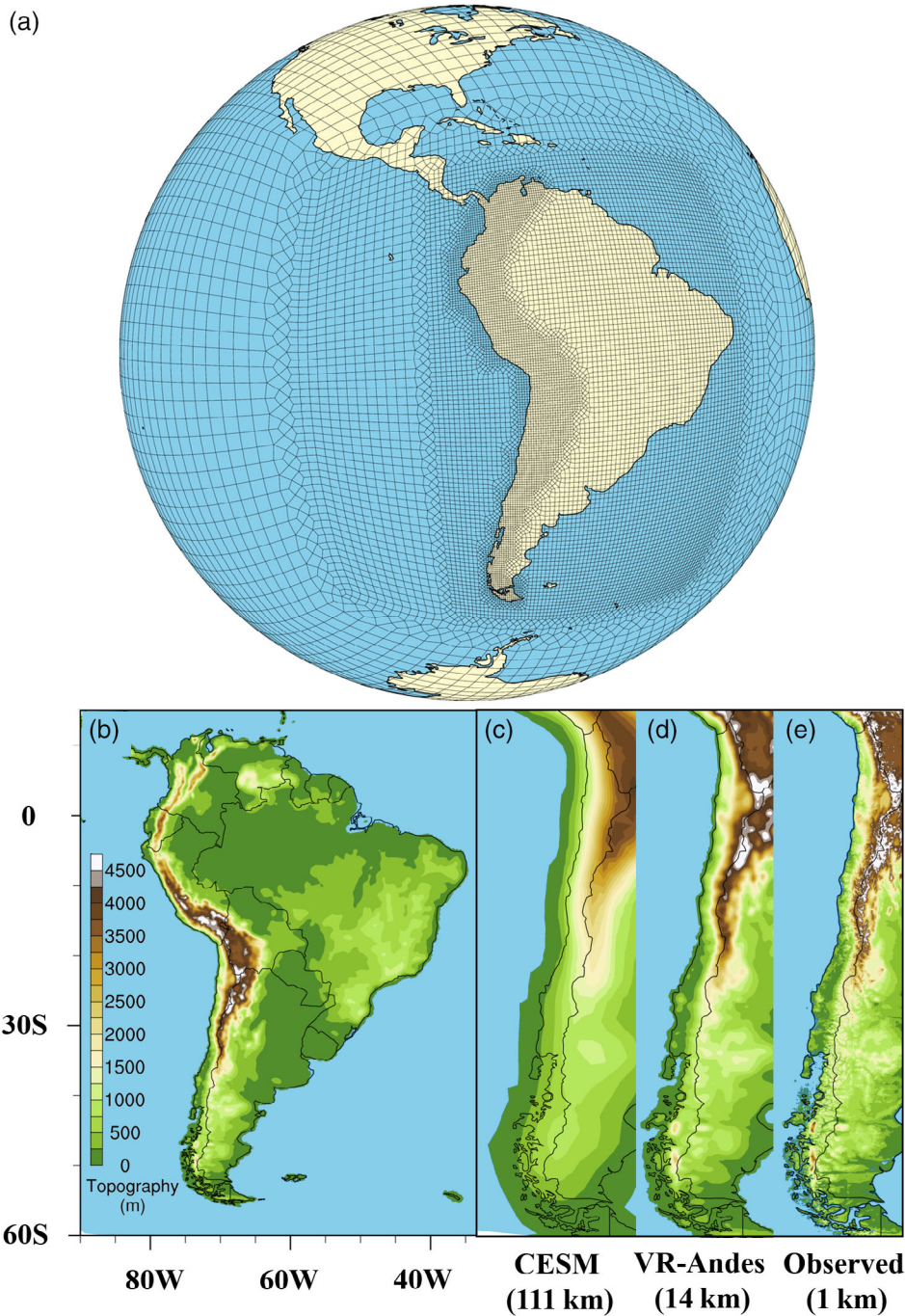


FIGURE 1 (a) Variable-resolution (VR) cubed-sphere grid developed for this study and implemented into the Community Earth System Model (hereafter, VR-Andes). VR-Andes has a quasi-uniform 111 km (1.00°) global resolution, 55 km (0.50°), and 28 km (0.25°) transition refinement regions over the East Pacific and South America, and an innermost refinement region of 14 km (0.125°) over the South American Andes. (b) South American VR-Andes topographic resolution. Comparison of Chilean topographic representation across a standard CESM resolution [111 km; Panel (c)], the resolution used in VR-Andes [14 km; Panel (d)], and a 1 km digital elevation model from the U.S. Geological Survey [GTOPO30; Panel (e)]

temperature and precipitation and convey the interactions of these changes via the Köppen–Geiger climate classification system across South America (Section 3.2.1). This is followed by a more nuanced assessment focusing on Chile, with the specific aim to explore the impacts of a warming climate on the Chilean cryosphere (Section 3.2.2). Next, we discuss the value-added by and limitations of the VR-Andes simulations within the broader literature (Section 4). We conclude with key findings as well as suggestions for future research needs (Section 5).

2 | DATA AND METHODS

2.1 | Community Earth System Model

The Community Earth System Model (CESM) is a state-of-the-art model with representations of the atmosphere, land-surface, ocean, land- and sea-ice, and river transport that can be either stand-alone or fully-coupled (Danabasoglu *et al.*, 2020). To capitalize on the regional telescoping capabilities within CESM (Zarzycki *et al.*, 2014b), we utilize the Community Atmosphere

Model (CAM) with the spectral element dynamical core (CAM-SE) version 5.4. Notable changes from CAM5.0-SE (default in CESM1.0) to CAM5.4-SE are related to a new floating Lagrangian vertical coordinate and, important to this study, a prognostic microphysics scheme that enables the advection of raindrops and snowflakes between grid cells (Gettelman *et al.*, 2015; Gettelman and Morrison, 2015), further discussed in Rhoades *et al.* (2018).

The variable resolution grids for this study (Figure 1) were generated with SQuadGEN (Ullrich, 2014) and incorporated in all model components of CESM used in this study, namely the atmospheric and land-surface models. Notably, the 28 km refinement domain in VR-Andes was designed according to the South American CORDEX (SA-CORDEX) regional climate simulations discussed in Solman *et al.* (2013) and Solman (2013).

We couple CAM5.4-SE with the Community Land Model (CLM) version 5.0 (Lawrence *et al.*, 2019). Compared with CLM4.0, CLM5.0 offers improved performance across a wide-range of the International Land Model Benchmarking (ILAMB) metrics (Collier *et al.*, 2018). Overall, CLM5.0 preliminary results highlight that processes shaping the ecosystem and carbon cycle are markedly improved while drawbacks were seen in surface runoff and water storage anomalies (Lawrence *et al.*, 2019). Of interest to this study's focus on the Chilean Andes, which stores large amounts of water in seasonal and perennial snowpack as well as glaciers, are the major enhancements to the CLM snow model (van Kampenhout *et al.*, 2017). These enhancements stem from augmenting the previous over-dependence on temperature thresholds for snow density and the inclusion of wind transport effects. In addition, the snow model now has 12 layers and is not artificially constrained to 1,000 mm of snow water equivalent. This reduces potential sources of error in seasonal estimates of snowpack, especially in the high elevation and high latitude regions of the Andes. Forest canopies can now capture both rain and snow (Lawrence *et al.*, 2019). These updates, along with a new firn snow parameterization, were found to significantly enhance the simulation of land-ice in Greenland (van Kampenhout *et al.*, 2017).

Our VR-Andes simulations were run over a 31-year historical period spanning 1984–2014. One year of spin-up (all of 1984) was performed to ensure that the soil moisture in CLM5.0 reached equilibrium. To limit computational cost and ensure that important South American large-scale climate variability drivers were well represented, we ran our VR-Andes simulation with prescribed sea-surface temperature and sea-ice concentrations, following the protocols of the Atmosphere Model Intercomparison Project (AMIP; Gates *et al.*, 1999). Full chemistry and aerosol processes in CAM5.4 were turned

off and prescribed instead to reduce computational costs. To further capitalize on the 14 km horizontal resolution, we set CLM5.0 to satellite phenology mode and utilized the 5 km, year 2000, land-surface cover dataset (Figures S1 and S2). The dynamics time step, dictated by the finest-resolution domain, was 30 seconds and the physics time step was set to 450 s, one-fourth the default, to account for finer horizontal refinement and ensure tighter coupling with the dynamics time step. Given the aforementioned choices, the VR-Andes simulations performed at 4.7 simulated years per day using 100 nodes (dual-socket nodes, 18 cores per socket) on the National Science Foundation Cheyenne supercomputing facility [145,152 total cores with 2.3-GHz Intel Xeon E5-2697V4 (Broadwell) processors] and resulted in ~70 TB of data with most variables output at monthly frequencies and select variables at daily and 3-hourly. To project the climate of South America, we performed two 30-year simulations under the RCP8.5 scenario (Riahi *et al.*, 2011), plus 1 year of spin-up for each 30-year period (all of 2029 and 2069). One simulation spanned 2029–2059 and the other 2069–2099, respectively. For these simulations, the AMIP-style simulations used sea-surface temperatures and sea-ice from a fully coupled, bias-corrected CESM1.0 simulation analogous to Rhoades *et al.* (2017).

2.2 | Reanalysis datasets

To evaluate the performance of the VR-Andes historical simulation, we compared our results against five different surface temperature and six different precipitation reanalyses, akin to Solman *et al.* (2013) and Solman *et al.* (2013). After considering the temporal period of record, variety of available observations, and spatiotemporal resolution of reanalysis products, we converged on three monthly reanalysis products. These include the Climate Hazards Center InfraRed Precipitation with Station data version 2.0 (CHIRPS, precipitation), The Modern-Era Retrospective Analysis for Research and Applications version 2 (MERRA-2, temperature), and the University of Delaware (UDEL, temperature and precipitation). Further considerations were gleaned from studies like Condom *et al.* (2020) who show that CHIRPS provides reasonable satellite-based rainfall estimates in Chile and recommends its use for hydrological applications.

2.2.1 | Climate Hazards Centre InfraRed Precipitation with Station (CHIRPS)

CHIRPS has a spatial resolution of 0.05°, spans 1981–present and covers 50°S–50°N latitude across all

longitudes (Funk *et al.*, 2015). To generate precipitation estimates, CHIRPS combines in-situ measurements and satellite retrievals. The in-situ measurements range from 32,000 observations in the early-1980s to around 14,000 in the mid-2010s. Observations include the Global Historical Climate Network-Daily [GHCN-D; (Menne *et al.*, 2012)], Global Summary of the Day, Global Telecommunication System and Southern African Science Service Centre for Climate Change and Adaptive Land Management. Satellite-based retrievals are derived from five satellites that sample in the microwave and infrared wavelengths. To merge in-situ measurements with satellite retrievals, CHIRPS developers utilize local regression at every latitude and longitude using between one and three co-variables from the satellites and topography (e.g., elevation and slope). To account for bias, a five-station weighted-average ratio is combined with a station-by-station de-correlation distance.

2.2.2 | Modern Era Retrospective Reanalysis 2 (MERRA-2)

MERRA-2 spans 1980–present with 72 vertical levels (surface to 0.01 hPa) and a spatial resolution of 0.5° by 0.625° over the whole globe (Gelaro *et al.*, 2017). The Goddard Earth Observing System (GEOS) assimilation system produces the MERRA-2 reanalysis product. GEOS utilizes 15 different observational sources, primarily from aircraft and satellites, with up to 5 million observations every 6 hr. Bias correction is applied to these estimates and is tailored for each individual satellite sensor channel. Precipitation is corrected using a variable weighting between GEOS model-based estimates and gauge-based global precipitation products, particularly at low-to-mid latitudes. Recent modifications from MERRA to MERRA-2 include conservation of dry air mass and water balance.

2.2.3 | University of Delaware (UDEL) air temperature and precipitation

UDEL is a global, 0.5° degree resolution reanalysis that spans 1900–2014 (Willmott and Matsuura, 1995; Willmott and Robeson, 1995). To derive air temperature and precipitation, UDEL utilizes the Global Historical Climate Network Daily [GHCN-D; (Menne *et al.*, 2012)] and several spatial interpolation schemes. One scheme is called climatologically aided interpolation (CAI; Willmott and Matsuura, 1995). CAI leverages high-resolution, long-term average global fields to compute deviations at each station location which are then spatially interpolated

using a spherically based inverse-distance weighting method. This yield mean absolute errors lower than traditional methods (i.e., 1.3°C in heavily instrumented regions and 1.9°C in data scarce regions). However, because of the use of long-term averages in the interpolation, interannual variability is dampened. Another scheme utilizes a digital-elevation-model (DEM; Willmott and Robeson, 1995). Adding in the DEM-based interpolation method, specifically a mean environmental lapse rate of $6.5^\circ\text{C}\cdot\text{km}^{-1}$ for temperature, adds further improvement (i.e., accuracy increase of 35% in the continental United States, or mean absolute error of 0.38°C). In this study, we use the UDEL product that leverages both the CAI- and DEM-based methodologies.

2.3 | Dataset regridding and statistical analysis

VR-Andes simulations were re-gridded from their native unstructured grid to the original resolution of each of the reanalyses on a regular latitude-longitude grid and compared. Thus, comparison to MERRA-2 and UDEL were performed at 55 km and CHIRPS to 6 km, respectively. When comparing across VR-Andes simulations, we re-gridded each simulation to a regular latitude longitude grid of 14 km, the finest resolution employed over the Andes. Re-gridding was performed using the Earth System Modelling Framework (ESMF) Offline Re-gridding Weight Generator using the first-order conservative remapping procedures available in The NCAR Command Language (Version 6.6.2) (2020), particularly since many reanalyses comparisons were at coarser resolution than the native resolution of VR-Andes. To test statistical significance of differences between reanalysis and historical model output and between future and historical model output, we performed two-tailed Student's *t*-tests. We limit Type-1 errors in these significance tests by employing the False Discovery Rate (Benjamini and Hochberg, 1995; Wilks, 2016). For seasonal trend analyses, we performed linear regressions and calculated the significance of the trend using the nonparametric Mann-Kendall test (Hamed and Ramachandra Rao, 1998).

2.4 | Köppen–Geiger classification maps

Maps illustrating how climate change may lead to the spatial redistribution of historical climate regions are limited. One method to devise these maps is the Köppen–Geiger classification system (Köppen and Geiger, 1954), which splits all regions of the globe into five categories: equatorial, arid, temperate, cold, and polar. These regions

are then sub-divided based on annual and/or monthly precipitation and temperature thresholds and/or ranges (Kottek *et al.*, 2006; Chen and Chen, 2013; Rubel *et al.*, 2017; Beck *et al.*, 2018). Beck *et al.* (2018) presented the first global high-resolution maps of the Köppen–Geiger classification system for both historic and future climates. While several versions of the Köppen–Geiger climate classification have been developed, in this study, we followed the criteria detailed in Kottek *et al.* (2006). A detailed list of criteria based on temperature and precipitation indices is presented in Tables S1 and S2. Climatological monthly mean surface temperature and total precipitation for the historic, near-future, and end-century periods were obtained from the VR-Andes datasets to compute Köppen–Geiger climate classifications.

3 | RESULTS

3.1 | Historical climate

To assess the veracity of the VR-Andes simulations in representing the historical climatology of South America, we first compare the simulated seasonal climatologies of 2 m surface temperature and accumulated precipitation to a diverse range of reanalyses (Figures 2 and 3). We focused our analyses on austral winter, June–July–August (JJA), and austral summer, December–January–February (DJF). Notably, there are well-known in-situ measurement gaps in the South American Andes. Although there are 14,595 meteorological and hydrological monitoring stations throughout the Andes, 60% are in Colombia and $\approx 70\%$ of the stations are between 0 and

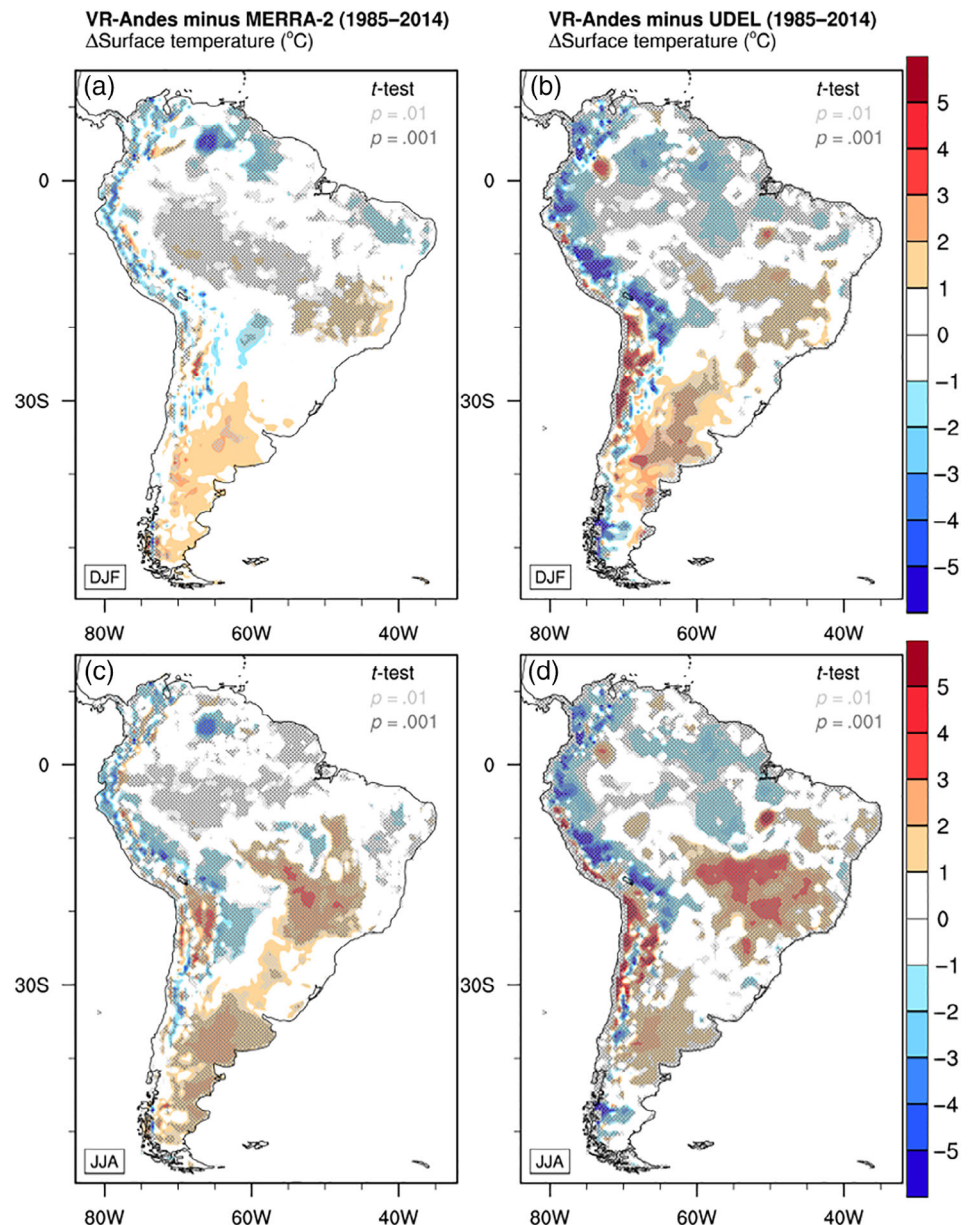


FIGURE 2 1985–2014 Climatological differences of 2 m surface temperature between VR-Andes and MERRA-2 [Panels (a) and (c)] or UDEL [Panels (b) and (d)] for austral summer (DJF, top-row) and winter (JJA, bottom-row). Stippling indicates statistically significant differences in seasonal averages using the student *t*-test and corrected for Type-I error using the false discovery rate (FDR, Benjamini and Hochberg (1995); Wilks (2016)) at *p*-values of .01 (light grey) and .001 (dark grey)

2,000 m elevation (Condom *et al.*, 2020). This undoubtedly influences any station-based reanalysis estimates of 2 m surface temperature and precipitation, especially at high elevations. This motivated our choice to use reanalyses that primarily rely on either station-based (e.g., UDEL) and/or satellite-based measurements (e.g., CHIRPS).

VR-Andes simulated a historical climate average of 23.1°C over South America in austral summer (Figure 4). This is slightly warmer than MERRA-2 (22.9°C) and cooler than UDEL (23.4°C), although with important differences observed in the high-altitude Andes and the western Amazon area (Figure 2). The austral winter average temperature simulated by VR-Andes was 19.1°C, which is 0.5°C warmer than MERRA-2 and nearly identical to UDEL (Figure 4). Differences in most regions are not statistically significant

or are in regions that have sparse in situ networks. Uncentred Pearson product-moment coefficient of linear correlations between VR-Andes and the reanalyses were nearly 1 for both austral winter and summer. Similar to JJA, disagreement was largest in the highest elevations of the Andes, over the Amazon, and portions of coastal Argentina (Figure 4). These results are consistent with the SA-CORDEX multi-model ensemble discussed in Solman *et al.* (2013) and Solman (2013), in which a similar cold bias in the highest elevations of the Andes in both DJF and JJA was found. However, VR-Andes biases are more localized in the Andes, likely due to more refined model resolution, and lower over most regions. Importantly, our comparison of VR-Andes is for a single-model simulation against two reanalyses, independently, whereas Solman *et al.* (2013) and Solman (2013) compared a multi-model ensemble

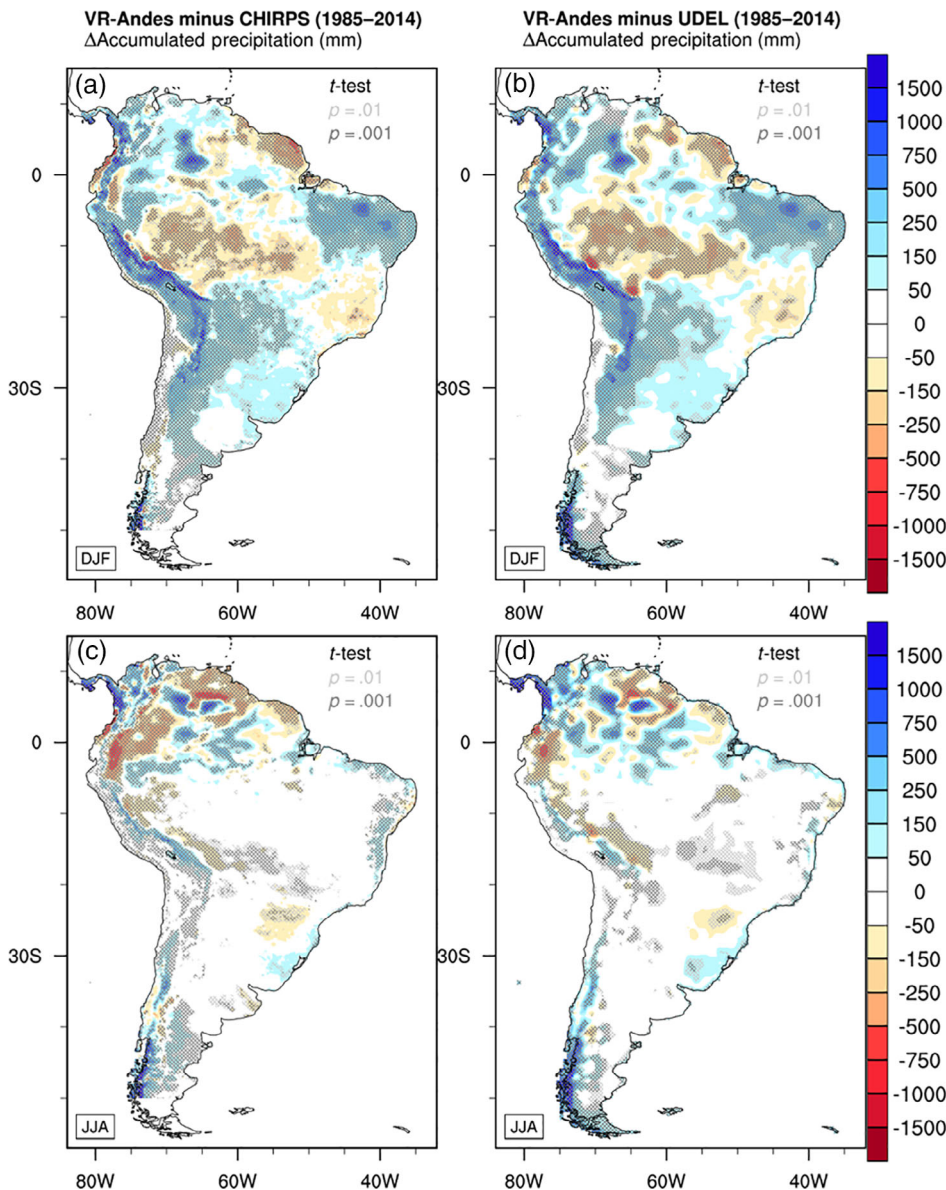


FIGURE 3 1985–2014 Climatological differences of accumulated precipitation between VR-Andes and CHIRPS [Panels (a and c)] or UDEL [Panels (b and d)] for austral summer (DJF, top-row) and winter (JJA, bottom-row). Stippling indicates statistically significant differences in seasonal averages using the student *t*-test and corrected for Type-I error using the false discovery rate (FDR, Benjamini and Hochberg (1995); Wilks (2016)) at *p*-values of .01 (light grey) and .001 (dark grey)

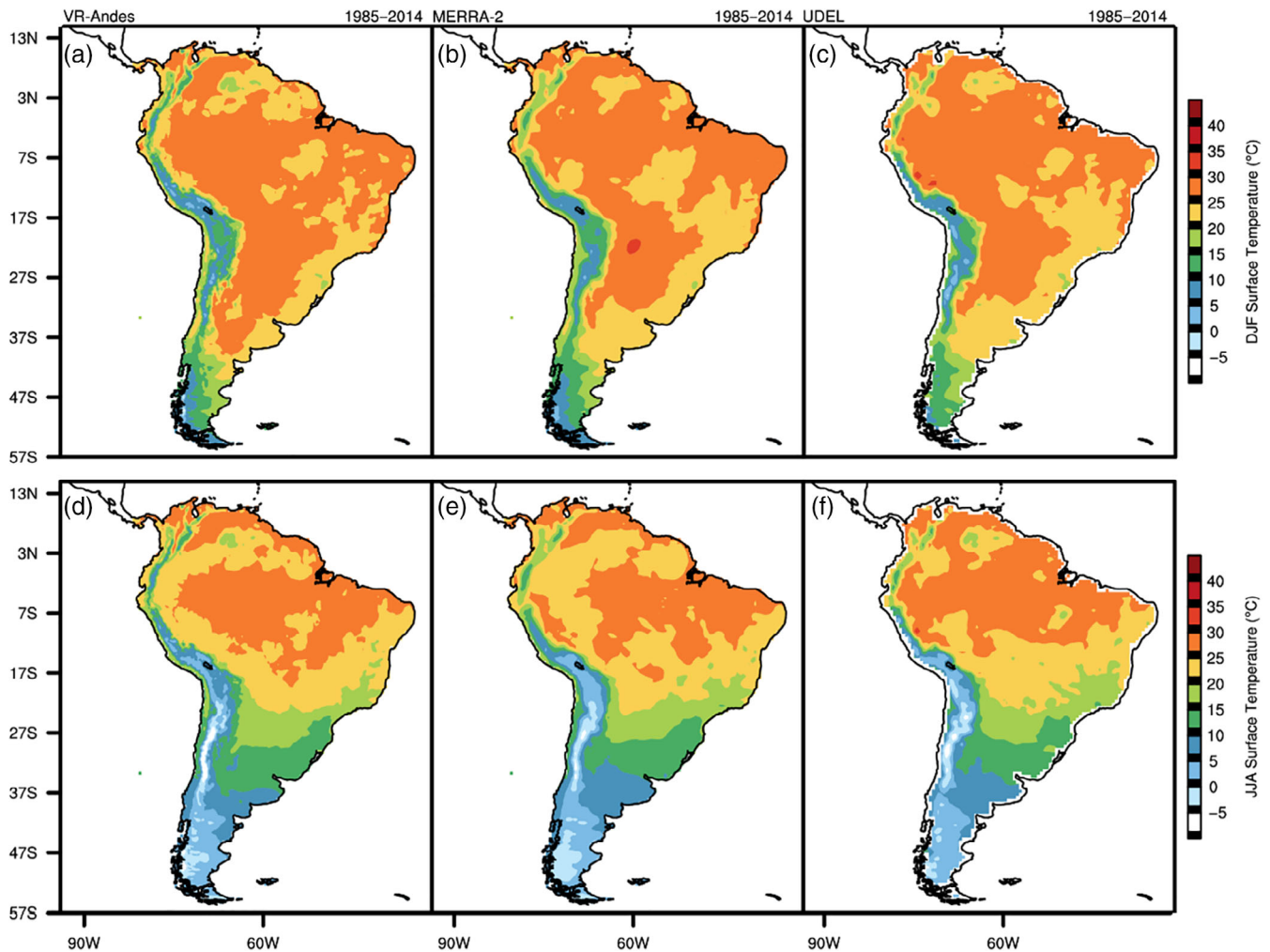


FIGURE 4 1985–2014 Climatological average 2 m surface temperature for VR-Andes [Panels (a and d)], MERRA-2 [Panels (b and e)], and UDEL [Panels (c and f)] for austral summer (DJF, top-row) and winter (JJA, bottom-row)

with a multi-reanalysis average. VR-Andes appears to perform reasonably well when compared against this multi-model ensemble average.

Overall, the magnitude and spatial pattern of austral winter accumulated precipitation are well represented by VR-Andes, yet larger differences are found during the austral summer (Figure 3). Differences are maximized in DJF when precipitation is dominated by mesoscale convection and minimized in JJA when synoptic-scale systems dominate (e.g., extratropical cyclones and associated atmospheric rivers). For both seasons, estimated precipitation has statistically significant differences compared to either CHIRPS or UDEL (Figure 5). However, DJF (JJA) un-centred Pearson product-moment coefficient of linear correlations between VR-Andes and UDEL and CHIRPS were very similar at 0.90 and 0.92 (0.86 and 0.91), respectively. For the entire South American region, during DJF (JJA), we observed a

mean precipitation difference of 223 (66) and 251 (97) mm between CHIRPS and UDEL, respectively. Compared with Solman *et al.* (2013) and Solman (2013), a general improvement in simulated precipitation occurs in JJA but is less apparent in DJF. The results from the SA-CORDEX ensemble identified a positive precipitation bias (about 50%) over south-eastern Brazil and Uruguay during the austral winter (Solman *et al.*, 2013) while VR-Andes estimates closely resemble the total mean winter precipitation for SACZ and LPB Regions (Figure 6). During the austral summer (DJF), VR-Andes tends to overestimate the total precipitation in about 8% in contrast to an underestimation of about 20% previously reported by Solman *et al.* (2013) for northern South America. A follow-up study that evaluates the potential precipitation drivers and biases during JJA (e.g., extratropical cyclones and atmospheric rivers) and DJF (e.g., convective precipitation) is planned.

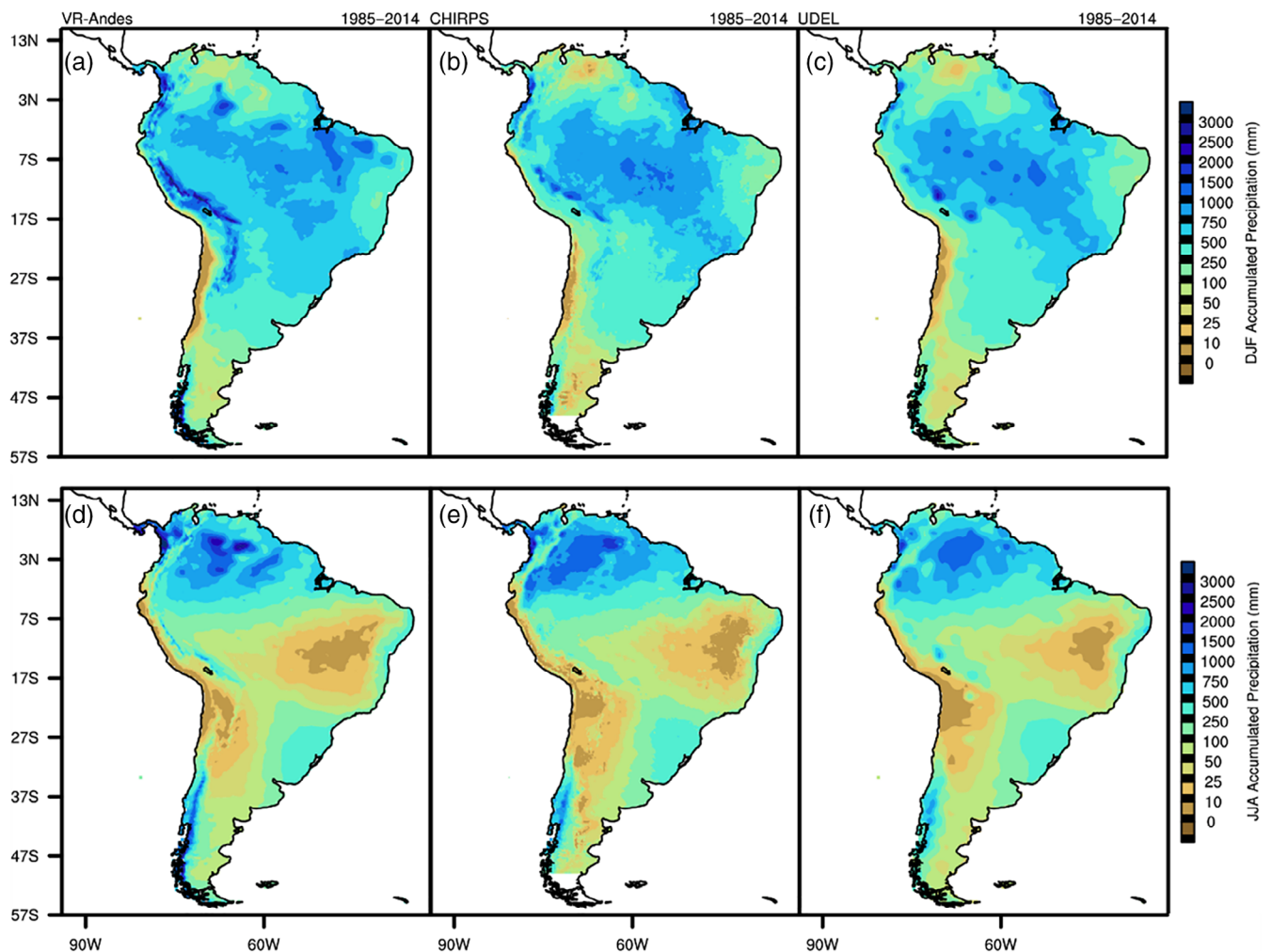
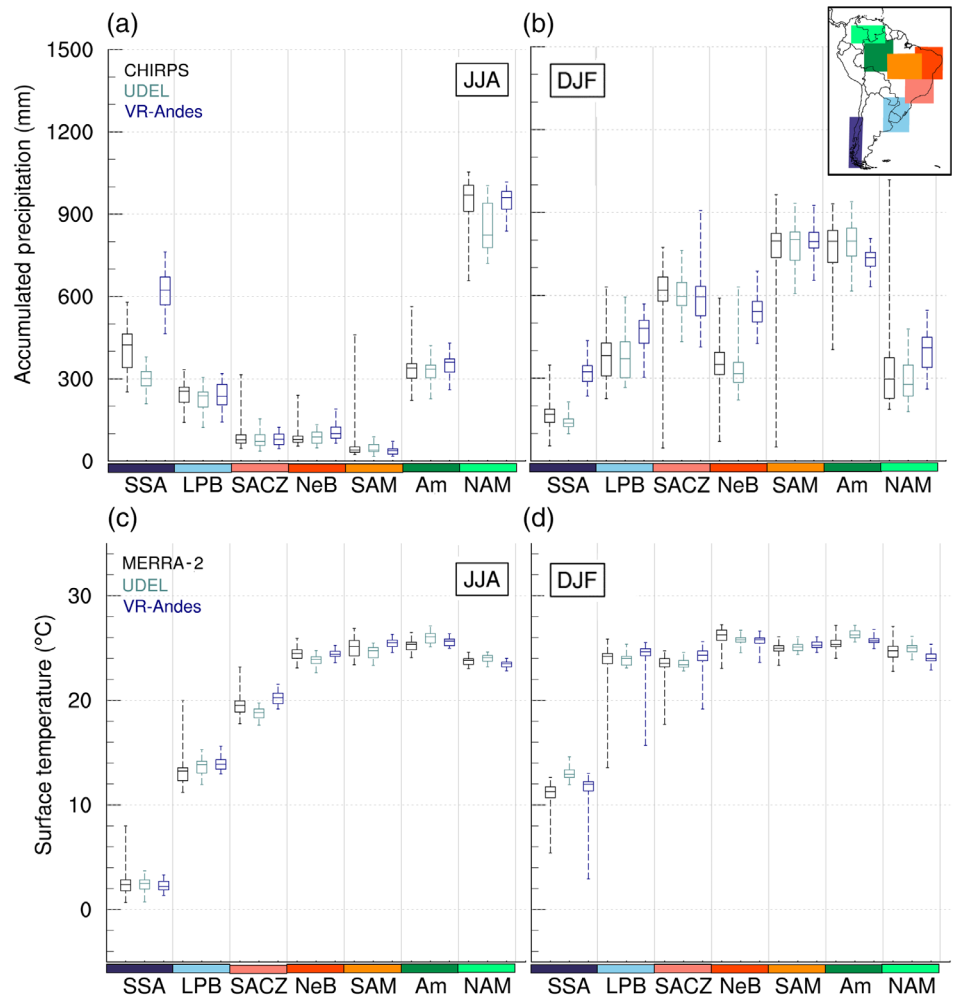


FIGURE 5 1985–2014 Climatological average accumulated precipitation for VR-Andes [Panels (a and d)], CHIRPS [Panels (b and e)], and UDEL [Panels (c and f)] for austral summer (DJF, top-row) and winter (JJA, bottom-row)

To further evaluate VR-Andes historical simulation skill relative to the three reanalysis datasets, we generated box-and-whisker plots for average austral winter and summer accumulated precipitation and 2 m surface temperatures using the seven South American subregions described in Falco *et al.* (2019) (Figure 6). These regions sample different portions of South America that are influenced by key regional atmospheric circulations (e.g., South American Monsoon and South American Low-Level Jet) and large-scale patterns (e.g., South Atlantic Convergence Zone) that shape the heterogeneity of the South American hydroclimate. For six of these seven regions, interquartile ranges in austral winter accumulated precipitation overlap with reanalyses. The sole mismatch was found in the subtropical South American (SSA) region where VR-Andes precipitation was larger than either reanalysis estimate. Notably, the interquartile ranges of CHIRPS and UDEL did not overlap for this

region. A consistent positive precipitation biases in SSA has been reported in previous regional and global climate model analysis (Falco *et al.*, 2019; Díaz *et al.*, 2021). As such, the SSA region will be explored in further detail in a follow-up study, namely to explore the role of atmospheric rivers in driving precipitation totals (Viale *et al.*, 2018). More disagreement in VR-Andes relative to reanalysis dataset estimates of accumulated precipitation was found in austral summer throughout South America. Three of the seven region's interquartile ranges did not overlap, specifically the SSA region, La Plata Basin (LPB) and northeastern Brazil (NeB), with VR-Andes precipitation totals higher than either CHIRPS or UDEL. These results contrast previous studies showing a negative austral summer precipitation bias for LPB, yet the bias found for the NeB region seems uncertain when compared to other modelling efforts (Solman *et al.*, 2013; Solman, 2016; Falco *et al.*, 2019). Seasonal average 2 m surface temperature had

FIGURE 6 Historical (1985–2014) austral winter (JJA, Panels a and c) and summer [DJF, Panels (b and d)] seasonal average box-and-whisker plots (i.e., minimum, 25th percentile, median, 75th percentile, and maximum) for seven South American subregions introduced in Falco *et al.* (2019) and indicated in each column using a corresponding colour bar to the map figure in the upper right. These regions include subtropical South America (SSA; navy blue), La Plata Basin (LPB; light blue), South Atlantic Convergence Zone (SACZ; salmon), northeast Brazil (NeB; orange-red), South American Monsoon (SAM; orange), Amazon (Am; green), and North American Monsoon (NAM; light-green)



less disagreement between VR-Andes and reanalysis datasets. VR-Andes interquartile ranges overlapped with at least one reanalysis dataset across all seven regions for both austral winter and summer.

Classification systems like the Köppen–Geiger provide intuitive ways to understand the interactions between precipitation and temperature. In comparison to previous Köppen–Geiger historical estimates, VR-Andes generally depicts similar patterns over South America (Figure 7). However, VR-Andes differs in several ways, particularly in the Andes. The Tundra, or Alpine, climate category (sub-climate of Polar), corresponding to climate conditions of at least 1 month of average temperature high enough to melt snow ($>0^{\circ}\text{C}$) and no month where mean temperatures are above 10°C , is markedly different. Although Tundra climates are expected to be found over the highest elevations of the Andes, particularly in mid-latitudes, this is generally not found in Beck *et al.* (2018). This could result from limited observational records within those areas and almost certainly results from the coarse resolution of the climate simulations that were used to construct those Köppen–Geiger maps.

3.2 | Future climate

3.2.1 | South America

Near-future and end-century changes in temperature and accumulated precipitation over South America are shown in Figures 8 and 9. By near future, South American austral summer is expected to follow the warming trend observed and projected by previous climate studies (Marengo *et al.*, 2010, 2012; Solman *et al.*, 2013; Sánchez *et al.*, 2015; Bozkurt *et al.*, 2019; Díaz *et al.*, 2021). Summer temperatures, on average, are expected to increase up to $+2.1^{\circ}\text{C}$ by mid-century and reaching $+4.3^{\circ}\text{C}$ by the end of the century (Figure 8). Precipitation changes are heterogeneous across the South American region. During austral summer, a clear drying trend is projected for the northwest and southwest regions of the continent, the Amazon region to the east of the Andes and the south of Brazil. A summer increase in precipitation is projected over the Northern windward Andes, Northeast Brazil, and La Plata Basin regions. In austral winter, slightly wetter conditions are expected over the highest peaks of

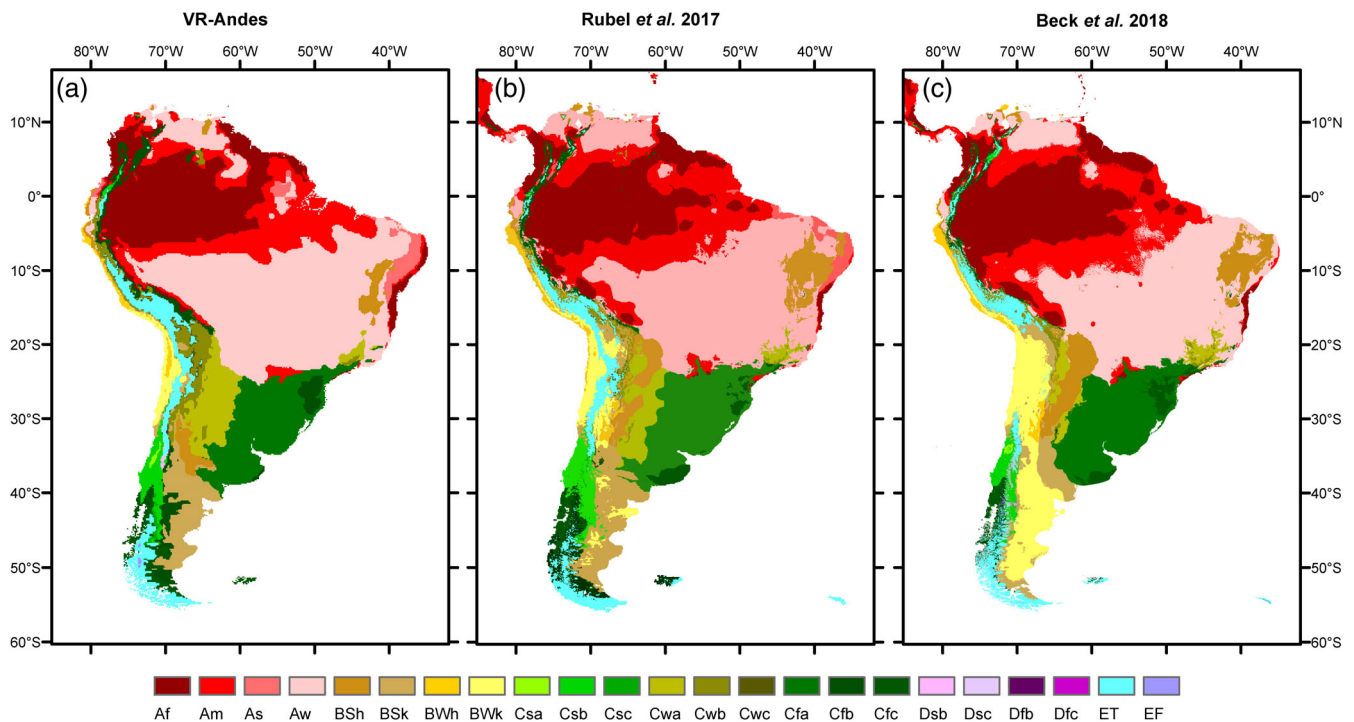


FIGURE 7 South American Köppen-Geiger climates simulated by VR-Andes over 1985–2014 [Panel (a)] and compared with two state-of-the-art Köppen-Geiger estimates, Rubel *et al.* (2017) [Panel (b)] and Beck *et al.* (2018) [Panel (c)]. Climates are given in letter-based categories using climatological monthly averages following the nomenclature from Köppen and Geiger (1954). For more information on how each letter-based category is computed, please see Tables S1 and S2. The colour scheme follows Kottek *et al.* (2006)

the Andes in central Chile, the western region of Colombia, southeast Brazil, and the western Patagonia region (Figure 9). Winter drying trends are projected for the southern Chile and areas over northeastern South America.

Regions of more notable climate changes emerge in austral winter systematic wetting or drying occurs with indicate amplified warming from the near future to end-century. Specifically, most of central South America and, in particular, the Andes show an amplified warming signal, as hypothesized in Pepin *et al.* (2015). Chile has one of the more unique changes in accumulated precipitation trends across South America with a meridional dipole in precipitation change projected. From 25°S to 55°S latitude, the climate is projected to become wetter in the northernmost regions, drier over the central and southern areas, and wetter over the southernmost regions. The region projected to become drier has also been at the epicentre of an ongoing Chilean megadrought (Boisier *et al.*, 2018; Garreaud *et al.*, 2020).

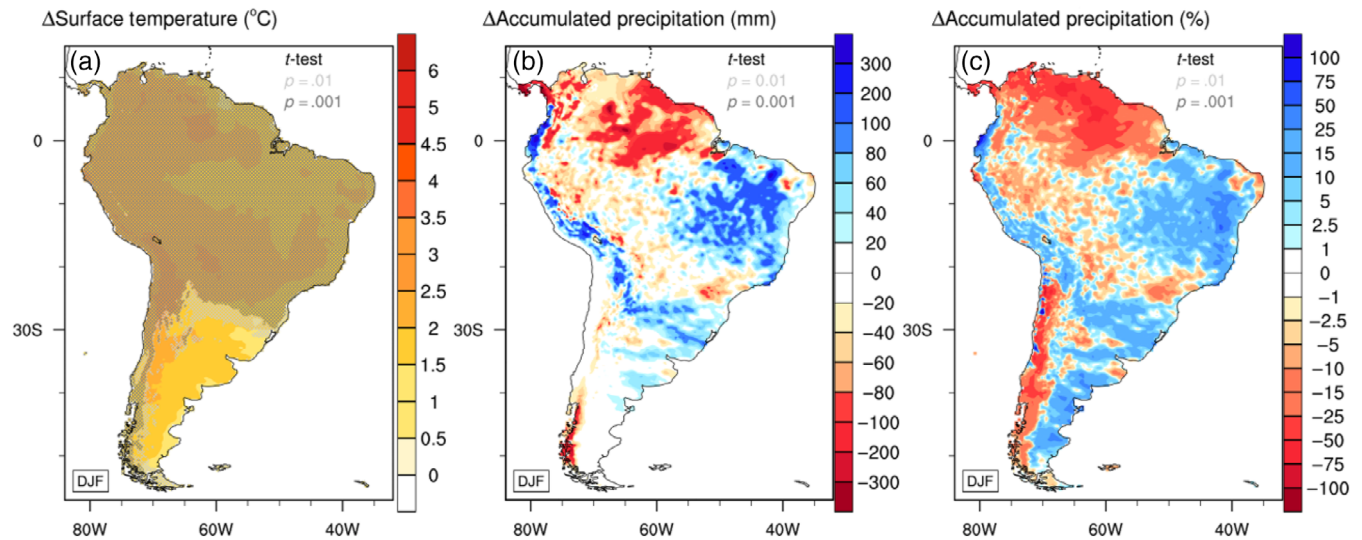
The interactions between changes in precipitation and temperature can be illustrated by using Köppen-Geiger classification maps. Strikingly, future VR-Andes projections show that the Tundra climate will become virtually nonexistent over South America by the end of

this century (Figure 10). These changes are expected to largely impact the Andes and Patagonia glaciers, following the trends observed in the last few decades (Dussailant *et al.*, 2018). Another large change simulated by VR-Andes at end-century is a 15% decrease in the Tropical Rainforest climate, particularly in the northeastern coastal region of South America, where the Tropical Savannah might expand by 20%. However, the Tropical Rainforest climates in the northwestern to northern areas of South America appear more stable and could be considered a ‘*climate refugia*’. The increase in surface area by the Arid Steppe Hot climate type in Argentina and Desert conditions in Chile and Peru illustrates projected changes that will drastically impact those regions.

3.2.2 | Chile

We next focus our analysis over Chile to leverage the higher resolution output from the VR-Andes simulations. Bozkurt *et al.* (2019) highlighted the expected added value from higher resolution simulations over this country given its complex topography and the wide range of climate conditions that occur there. The heterogeneous response of precipitation (Figure 9) and desertification

2030 – 2059 change relative to 1985 – 2014 | Austral Summer (DJF)



2070 – 2099 change relative to 1985 – 2014 | Austral Summer (DJF)

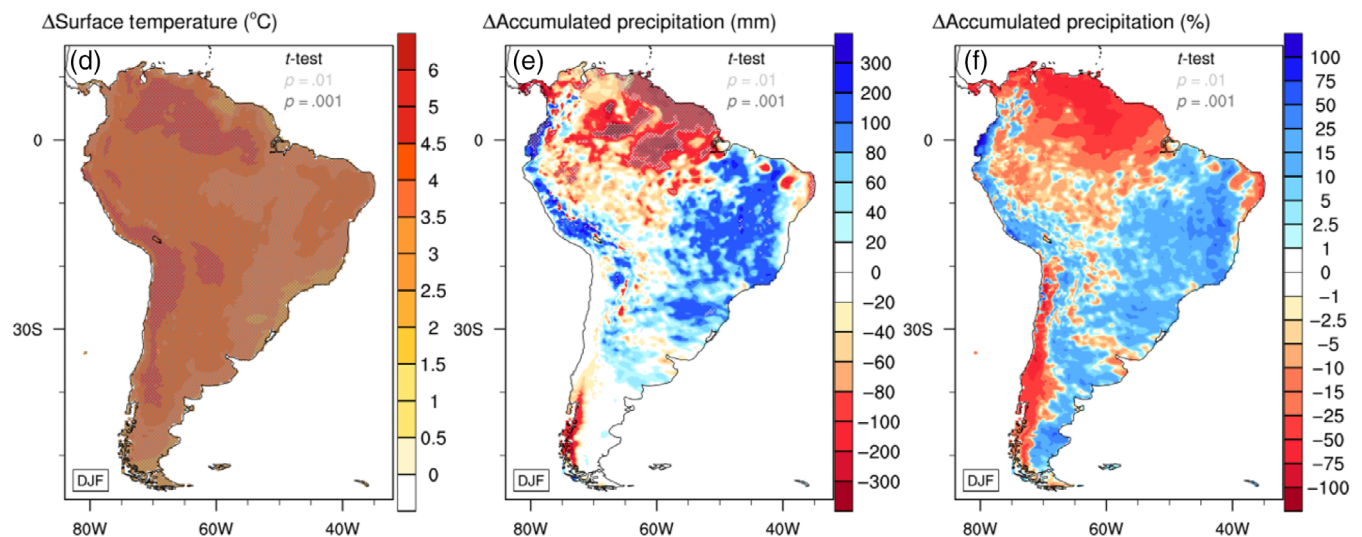
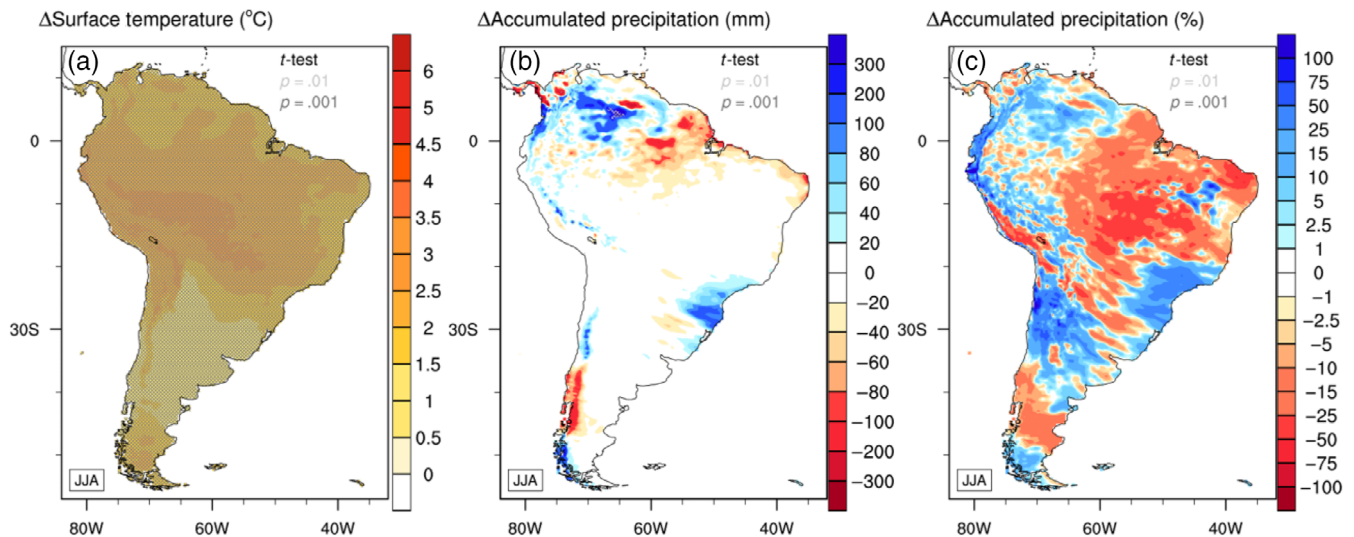


FIGURE 8 2030–2059 [Panels (a–c)] and 2070–2099 [Panels (d–f)] Climatological differences of 2 m surface temperature [Panel (a and d)], accumulated precipitation [Panel (b and e)] and percent changes in accumulated precipitation [Panel (d and f)] from the historical VR-Andes simulation (1985–2014) for austral summer (DJF). Stippling indicates statistically significant differences in climatologies based on seasonal average student t -test and corrected for Type-I error using the false discovery rate (FDR, Benjamini and Hochberg (1995); Wilks (2016)) at p -values of .01 (light grey) and .001 (dark grey)

(Figure 10) illustrate some of the projected climate changes. Over its long (4,500 km) and narrow (350 km) expanse, Chile has some of the highest mountain peaks in the world, one of the most agriculturally productive valleys, and a thriving coastal community. In addition, about one-third of Chile's population is located in its capital city, Santiago. Santiago is largely dependent on water supply provided by a few headwater basins, most importantly the Maipo basin that supports up to 80% of the potable water supply to the more than 5 million inhabitants (Undurraga *et al.*, 2020). Many Chilean watersheds are highly susceptible to flooding and drought, with

water resource infrastructure highly impacted by sediment accumulation events that decrease water quality (Saldías *et al.*, 2016; Garreaud *et al.*, 2017). Extreme sedimentation can even create widespread and at times prolonged water supply shortages (Andreoli *et al.*, 2012). These characteristics of Chile highlight the need for high-resolution modelling provided by the VR-Andes simulations. Given the wide range of climate conditions along Chile, we defined four regions: North, Central, South, and Austral. Overall, from the northern to southern regions it is projected that an increase in temperature (Figure 11) with less clear changes in annual

2030 – 2059 change relative to 1985 – 2014 | Austral Winter (JJA)



2070 – 2099 change relative to 1985 – 2014 | Austral Winter (JJA)

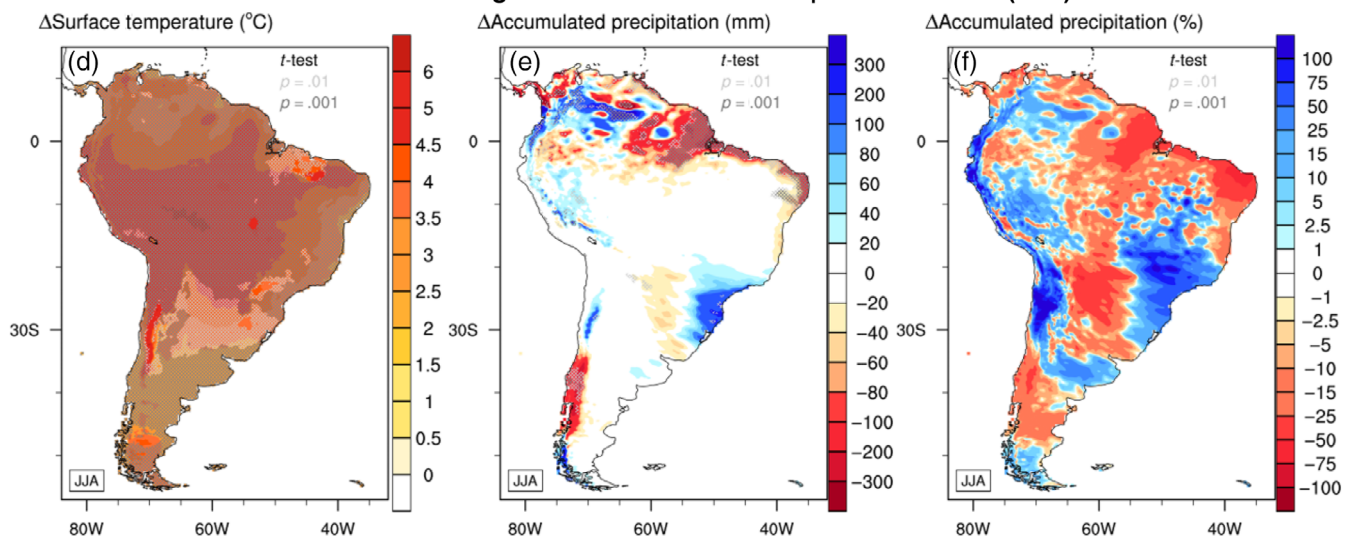


FIGURE 9 2030–2059 [Panels (a–c)] and 2070–2099 [Panels (d–f)] Climatological differences of 2 m surface temperature [Panels (a and d)], accumulated precipitation [Panels (b and e)] and percent changes in accumulated precipitation [Panels (d and f)] from the historical VR-Andes simulation (1985–2014) for austral winter (JJA). Stippling indicates statistically significant differences in climatologies based on seasonal average student *t*-test and corrected for Type-I error using the false discovery rate (FDR, Benjamini and Hochberg (1995); Wilks (2016)) at *p*-values of .01 (light grey) and .001 (dark grey)

precipitation (Figure 12) will occur. However, given Chile's complex topography, considerable heterogeneity of conditions is found within each defined region. A non-significant trend in future Chilean-wide accumulated precipitation is found for both seasons. This holds across all four subregions of Chile as well (Figure 12). Notably, a systematic drying trend in JJA of $\sim 30\text{--}40\text{ mm}\cdot\text{decade}^{-1}$ is found in the southern region of Chile ($35^{\circ}\text{S}\text{--}40^{\circ}\text{S}$) and is consistent with the significant drying seen in the Bío Bío and Araucanía provinces of Chile (Figure 9). Conversely, a step-wise shift in mean JJA accumulated precipitation occurs over the northern region of Chile ($17^{\circ}\text{S}\text{--}$

27°S), coinciding with the non-significant increase in precipitation in the Atacama Desert as well as wetter and non-significant JJA conditions in the austral regions of Chile, likely due to enhanced interannual variability (Figure 9). Warming trends in Chile are spatially coherent and significant across both seasons with an increase of $0.4\text{--}0.6^{\circ}\text{C}\cdot\text{decade}^{-1}$. Regionally, warming trends are greatest at near future and diminish at end-century in JJA in the northern half of Chile ($17^{\circ}\text{S}\text{--}35^{\circ}\text{S}$), yet continually and significantly increase with time in the southern half of Chile ($35^{\circ}\text{S}\text{--}55^{\circ}\text{S}$; Figure 11). Across all time periods and regions, DJF

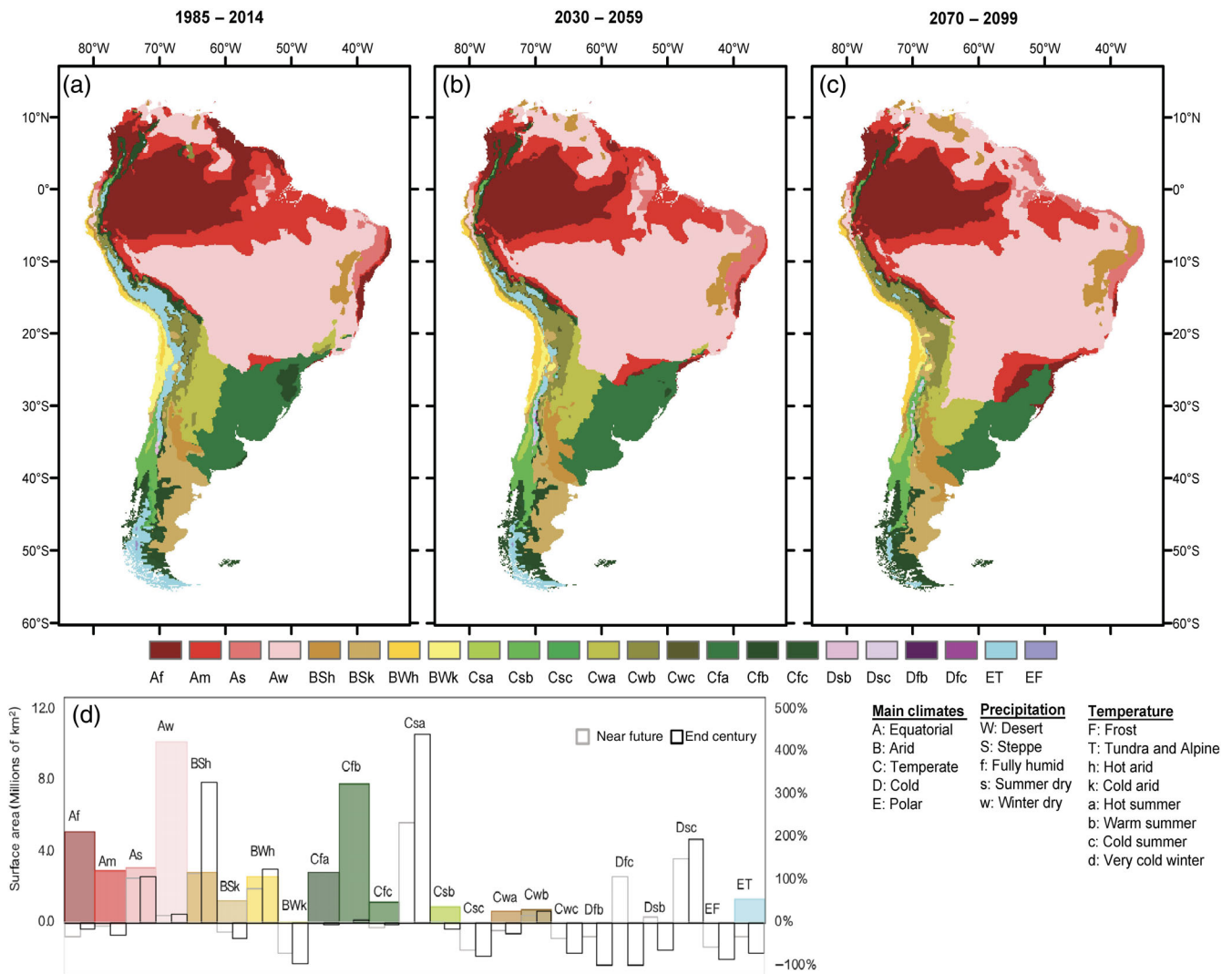


FIGURE 10 South American Köppen–Geiger (Koeppen, 2011; Rubel *et al.*, 2017) climates simulated by VR-Andes over 30-year historical [Panel (a)], near future [Panel (b)], and end-century periods [Panel (c)]. Climates are given in letter-based categories using climatological monthly averages following the nomenclature from Köppen and Geiger (1954). The colour scheme follows Kottek *et al.* (2006). Summary of total estimated surface area (coloured bars) per climate class and the corresponding projected change in percentage (clear bars) [panel (d)]. For more information regarding how each letter-based category is computed, please see Tables S1 and S2

temperature trends consistently and significantly increase (Figure 11).

To further contextualize JJA and DJF seasonal changes in Chile across the four subregions, Figure 13 provides box-and-whisker plots for historical, near future, and end-century seasonal averages from the VR-Andes simulations along with historical estimates from the three reanalyses. This is done to provide context between historical bias relative to future changes. Similar to the trend analysis, VR-Andes results indicate a systematic increase in spread in JJA accumulated precipitation from historical to near future to end-century in Austral Chile (42°S–55°S) and a downward shift in median accumulated precipitation in the southern region of Chile. This is

accompanied by a systematic warming whereby the minimum seasonal average temperature at end-century is above the maximum (75th percentiles) of historical (near future) simulations across most regions of Chile. The median accumulated precipitation does not change significantly in the Northern, Central, or Austral regions of Chile during DJF or JJA. Median precipitation declines with time in the Southern region during both seasons. The Southern region is projected to experience median accumulated precipitation that is below the lower quartile of the historic period compared to the near-future and end-century periods. The broadening interquartile range during JJA and DJF in the Austral region suggests an increase in precipitation variability. In all regions,

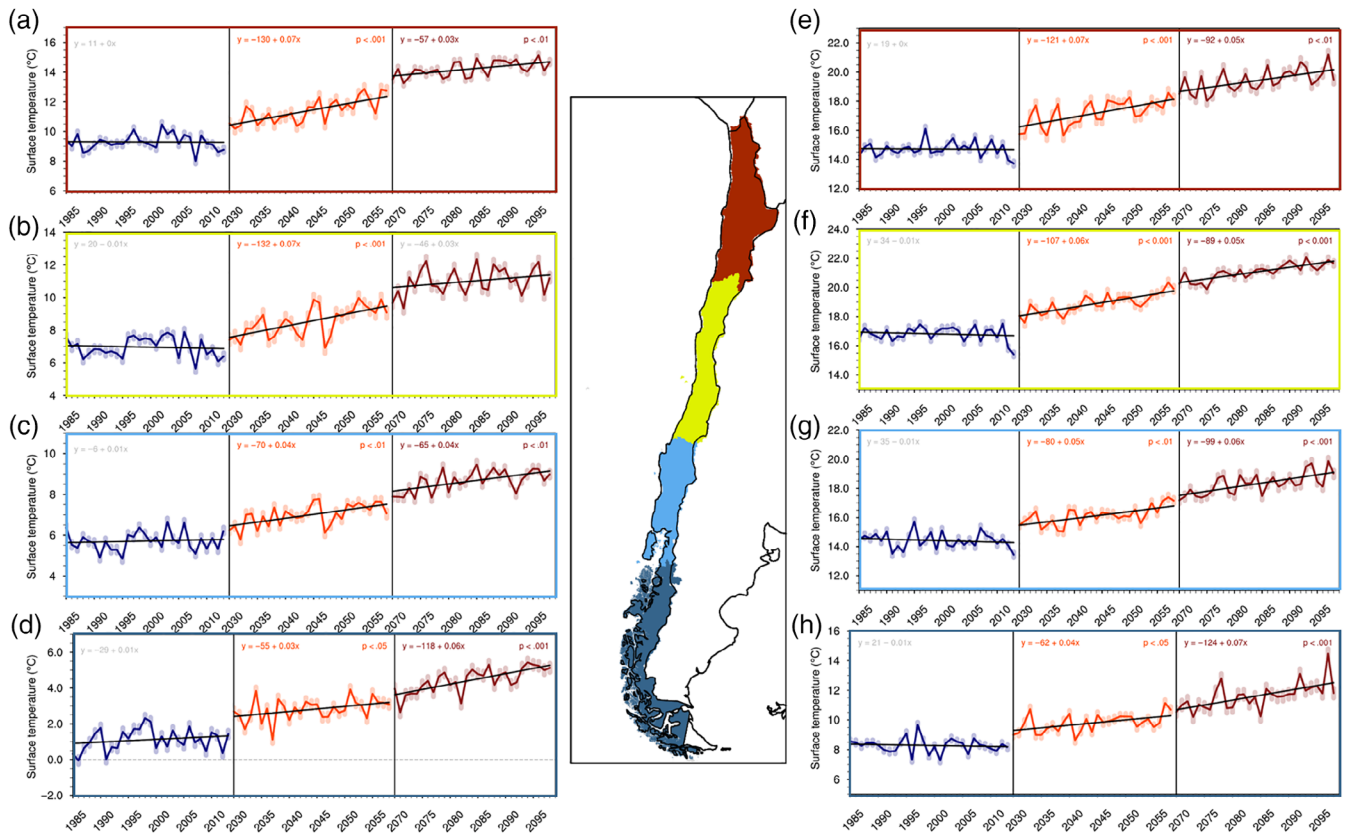


FIGURE 11 VR-Andes simulated 30-year seasonal trends for austral winter (JJA, left column) and summer (DJF, right column) 2 m surface temperature across four subregions of Chile (centre figure) for a historical (1985–2014, navy blue), near future (2030–2059, orange-red), and end-century (2070–2099, dark red) time period. Of note, 95% confidence intervals are shown via translucent lines for each season. If a trend line (black) is statistically significant at a p -value of, at least, .05 the linear equation in the upper left of each figure is emboldened and coloured. Chilean subregion trends are ordered from top-to-bottom as northern Chile [dark red, Panels (a and e)], central Chile [yellow, Panels (b and f)], southern Chile [light blue, Panels (c and g)], and austral Chile [dark blue, Panels (d and h)]

Figure 12 indicates future years may experience singular wet or dry seasons that exceed the range simulated for the historic period. Similar to JJA, DJF seasonal temperatures systematically increase from historical to near future to end-century (Figure 11).

We note there are discrepancies in historical seasonal averages estimated from the CHIRPS (provides accumulated precipitation) and MERRA-2 (provides temperature) reanalyses compared with the UDEL reanalysis (provides accumulated precipitation and temperature). More agreement is seen in accumulated precipitation (save for the austral region of Chile), yet a significant mismatch is found for temperature across most regions of Chile (southern region of Chile notwithstanding). Specifically, UDEL has a more constrained interannual variability compared with other reanalyses and VR-Andes for both accumulated precipitation and temperature. This is likely a result of its reliance on the climatologically aided interpolation (CAI) scheme to fill in situ network gaps (see Willmott and Matsuura (1995)). When comparing

MERRA-2 against VR-Andes we note that seasonal inter-quartile range overlap occurs for temperatures across all regions during both seasons. Similarly, VR-Andes and CHIRPS are largely in agreement for all regions in DJF and most regions in JJA, save for the southernmost Chilean regions. In these two regions, VR-Andes simulates significantly higher seasonal totals, which is consistent with climatological comparisons in Figure 5 as well.

Many regions of Chile are largely reliant on the storage of seasonal precipitation through the form of Andean snowpack, or snow water equivalent (SWE), and/or runoff from glacial melt. Changes in the seasonal cycle of Andean SWE and/or annual glacial mass balance provides a unique glimpse into the interactions between precipitation and temperature on both shorter (annual) and longer (decadal) timescales. For brevity, we focus our analysis of SWE estimates provided by the land-surface model (CLM5.0; Lawrence *et al.* (2019)) in the VR-Andes simulations between the end-century and the historic periods. A key result is the projected decline of the

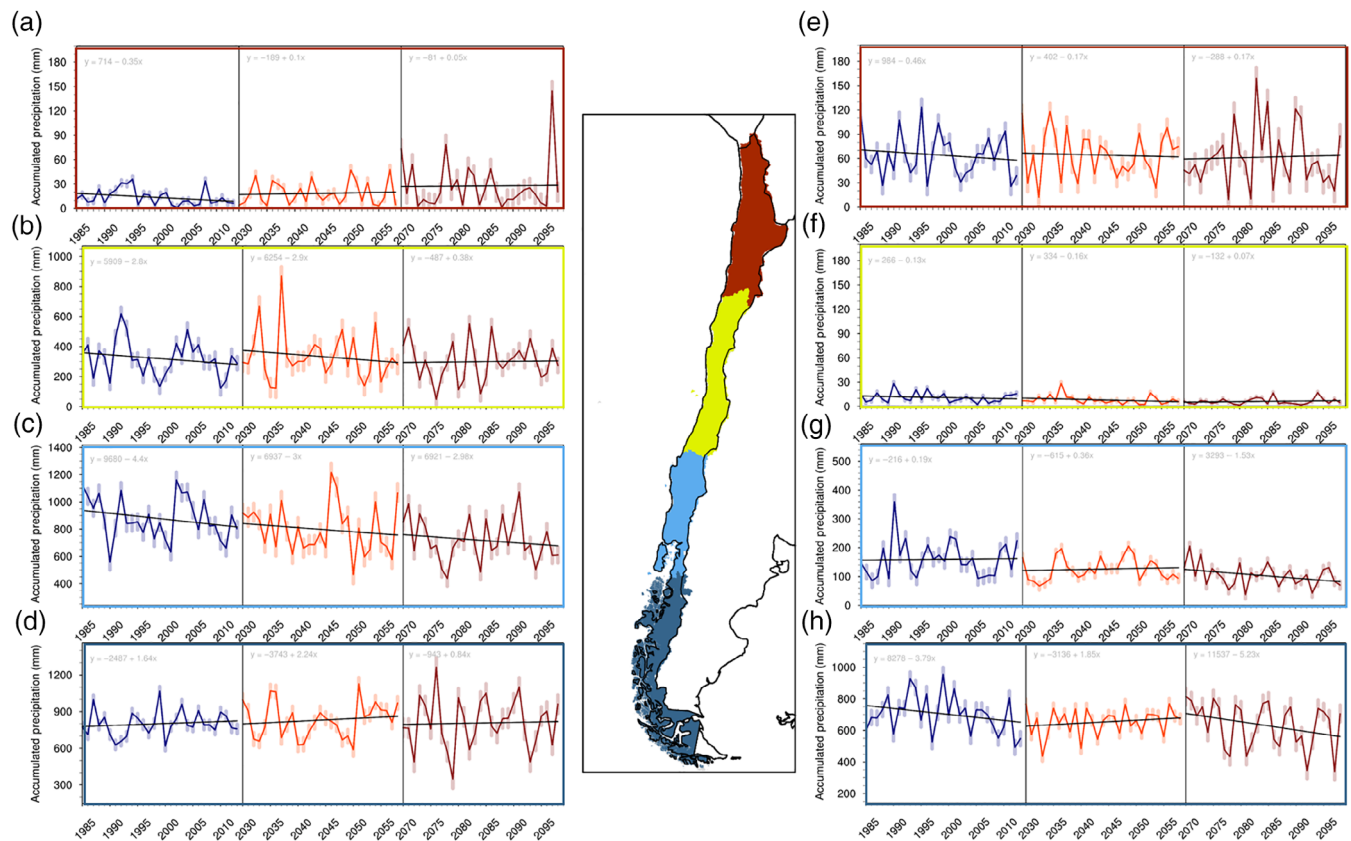


FIGURE 12 VR-Andes simulated 30-year seasonal trends for austral winter (JJA, left column) and summer (DJF, right column) accumulated precipitation across four subregions of Chile (centre) for a historical (1985–2014, navy blue), near future (2030–2059, orange-red), and end-century (2070–2099, dark red) time period. Of note, 95% confidence intervals are shown via translucent lines for each season. If a trend line (black) is statistically significant at a p -value of, at least, .05 the linear equation in the upper left of each figure is emboldened and coloured. Chilean subregion trends are ordered from top-to-bottom as northern Chile [dark red, Panels (a and e)], central Chile (yellow, Panels (b and f)), southern Chile [light blue, Panels (c and g)], and austral Chile [dark blue, Panels (d and h)]

Chilean cryosphere as interpreted through the first-order metrics of snowpack, temperature, and precipitation. The maximum amount of water stored in Chilean SWE during the extended austral winter (June–December; interpreted through the metric of median peak SWE) are projected to decline substantially throughout the range (Figure 14a–c). The largest declines will occur in the central Andes (≈ 200 – 600 mm; 35°S) and the austral Andes ($\geq 1,000$ mm; 47 – 52°S). The region between 38°S and 42°S is projected to become nearly snow-free in an average sense (median peak SWE = 0 mm) by the end of the century (Figure 14b). Smaller magnitude declines, particularly in the central Andes and at lower elevations in the austral Andes, are suggestive of the loss of seasonal snowpacks. The declining magnitude of peak SWE in the austral Andes, which exceeds 1,000 mm in some locations, are interpreted to indicate not only snowpack loss but also loss of perennial snow. Curiously, there is a projected increase in water stored as snow in the subtropical Andes on the order of 100–200 mm (Figure 14c). These

increases are likely the result of the projected increase in precipitation for this region (Figure 8e). Consistent with the smaller peak SWE magnitudes and broad warming trends over the region (Figure 8d), the median timing of annual peak SWE is projected to occur between one to more than 2 months earlier compared to the historic period (Figure 14d–f). There are indications of elevation-dependent warming as suggested by Pepin *et al.* (2015), with regions closer to the Andean crest undergoing the largest shifts (≥ 75 days) towards earlier peak SWE timing (Figure 14f).

Several mechanisms are likely responsible for driving the decline in peak SWE magnitudes and the earlier timing of peak SWE. For example, the annual number of days with minimum temperatures below 0°C are projected to decrease between 50 and 200 days (Figure 15a) with the largest decreases in the Northern, Southern, and northern Austral regions of the Chilean Andes and the smallest increases in the Central region. The number of days with maximum temperatures below 0°C is less

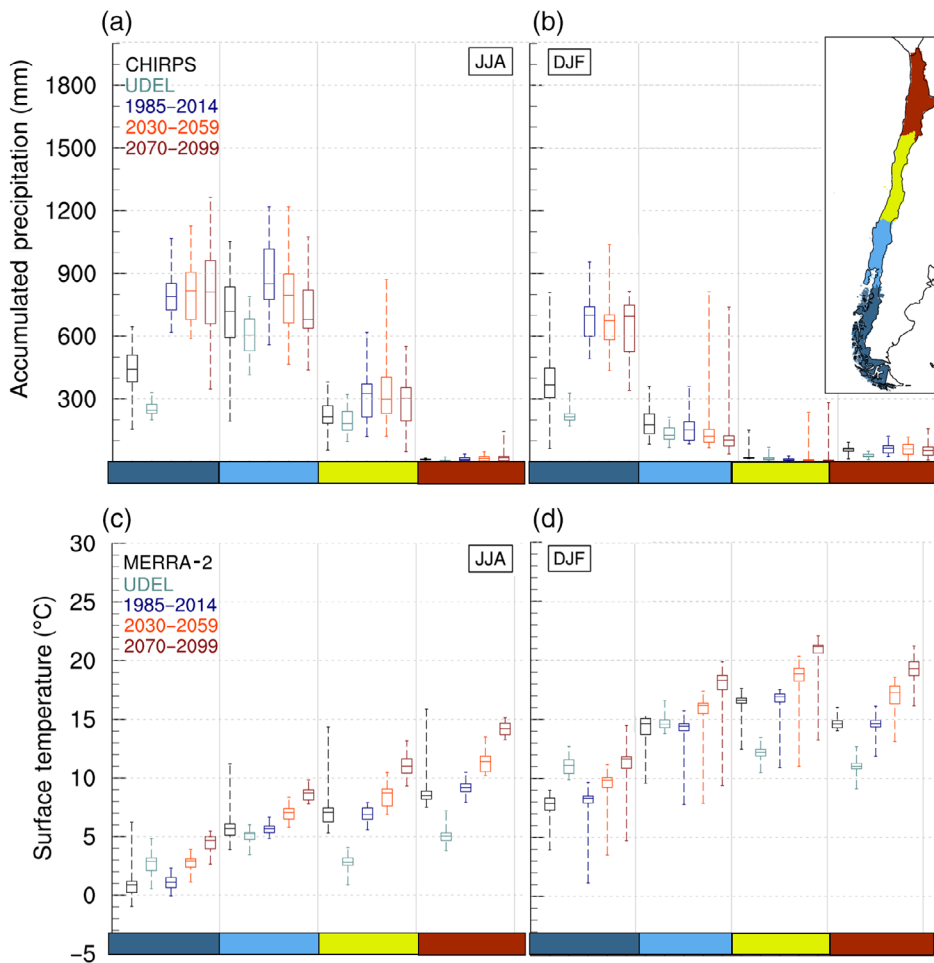


FIGURE 13 Austral winter [JJA, Panels (a and c)] and summer [DJF, Panel (b and d)] seasonal average box-and-whisker plots (i.e., minimum, 25th percentile, median, 75th percentile, and maximum) for the four Chilean subregions (indicated in each column using a corresponding colour bar to the map figure in the upper right) including northern Chile (dark red), central Chile (yellow), southern Chile (light blue), and austral Chile (dark blue) for historical (1985–2014) and future (2030–2059, 2070–2099) periods

widespread with the largest increases concentrated within the north central and especially the glaciated regions of the austral Andes (Figure 15b). Declines in the fraction of cool season (June–December) precipitation occurring at temperatures near freezing (when precipitation can still fall as snow due to the time it takes hydrometeors to melt [Jennings *et al.*, 2018]) are between 10 and 20% throughout much of the northern Andes (Figure 15c). The largest decreases ($\geq 30\%$) occur in the areas south of 45°S , with some regions of Austral Chile projected to have decreases of 50%. Throughout Chile, there are increases in the annual number of days projected to exceed the historical maximum temperature (Figure 15d). These increases are generally on the order of 150 days and are indicative of broad-scale warming. The changes are most notable in the Atacama region and in the glaciated regions of the southern Andes. In these regions, changes are upwards of 200 days (south) and 300 days (north). Consistent with earlier findings regarding the drying of the south-central region of Chile, dry days increase by 10–30 days (Figure 15e). We note a change in the temperature on cool season wet days Chile-wide on the order of $2\text{--}3^{\circ}\text{C}$ (Figure 15f). The largest

wet day warming is projected to occur in the northern and central regions, where warming is on the order of $4\text{--}5^{\circ}\text{C}$. Indications of elevation-dependent warming are shown by changes in cool season wet days, especially in the northern and central regions of the Chilean Andes.

4 | DISCUSSION

Our results are broadly consistent with other recent modelling efforts that project future climate change over South America. Both DJF and JJA show broad warming throughout South America ($+3\text{--}6^{\circ}\text{C}$ by end-century), yet precipitation trends are more heterogeneous and seasonally dependent with dipole-like responses in both the meridional and zonal directions. These two trends are consistent with the more qualitative South America-wide changes shown in Solman *et al.* (2013) and Solman (2013) (c.f. Figure 4) for DJF and JJA, yet are provided with more spatial granularity in the VR-Andes simulations. Cold biases are observed over the Andean region and warm biases are significant over southern Brazil, the Altiplanic region over Chile, Bolivia, Peru, and

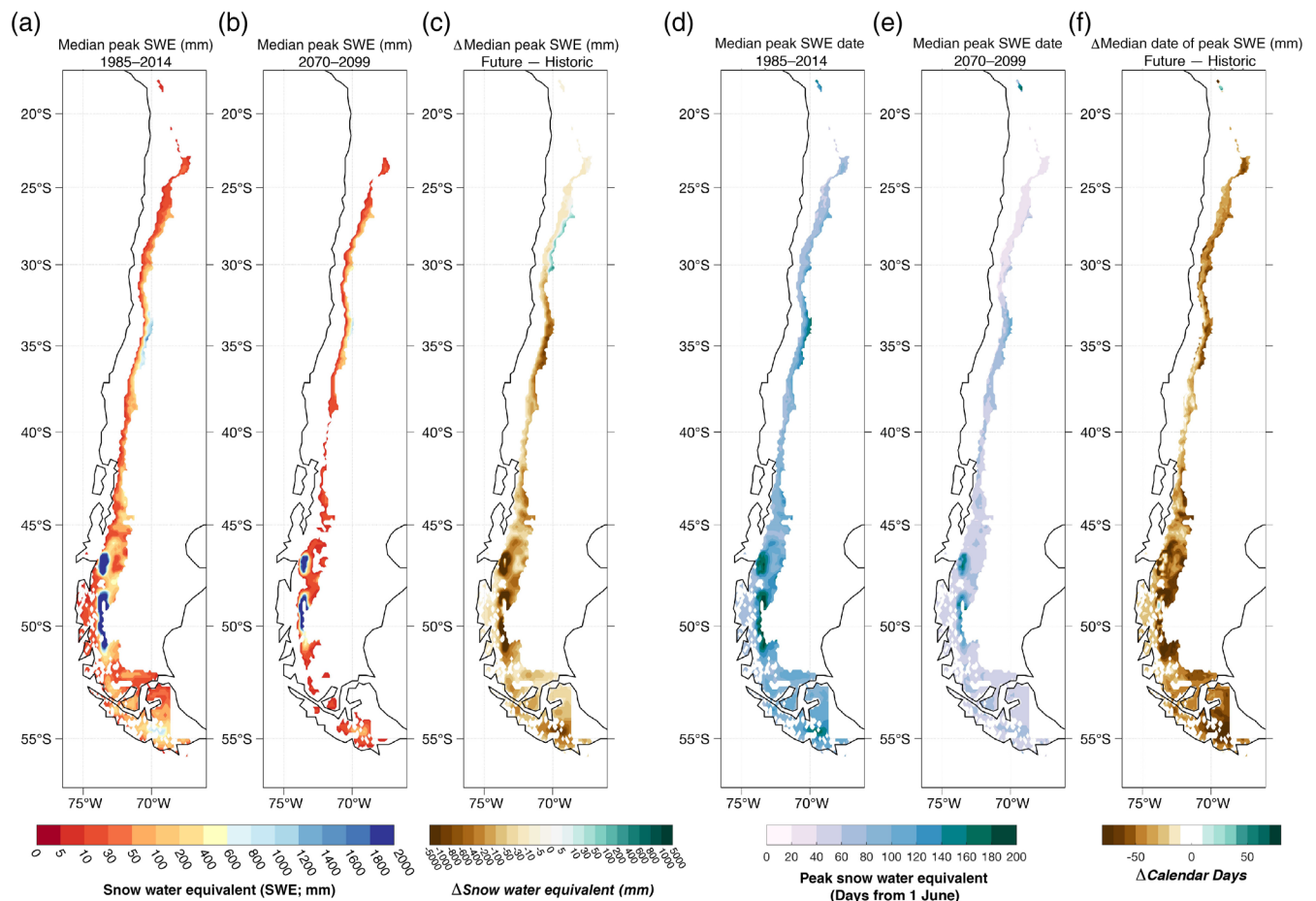


FIGURE 14 Historic [1985–2014; Panel (a)], future [2070–2099; Panel (b)], and the difference between future and historic [Panel (c)] of peak snow water equivalent (SWE) magnitude (mm). Historic [1985–2014; Panel (d)] and future [2070–2099; Panel (e)] timing of peak SWE starting from June 1. Change in timing of peak SWE between future and historic [Panel (f)]

Argentina, and the Argentinean Pampa. These temperature biases present patterns previously found by Falco *et al.* (2019), but overall those biases were slightly larger in magnitude compared to VR-Andes. Positive biases in accumulated precipitation are significant across all the Andes during summer within the tropical region and winter over the subtropical region. Wetter austral winter conditions are projected for the tropical, central, and southern-most Andes, the exit region of the Chaco jet, and Colombia into central Venezuela. The precipitation bias in this region is consistent with previous studies pointing the outstanding need of better characterizing the structure and dynamics of the east Pacific Intertropical Convergence Zone (ITCZ) as simulated in CESM (Woelfle *et al.*, 2019), as well as other General Circulation Models (GCM) (Adam *et al.*, 2018). Conversely, drier conditions are projected in the VR-Andes simulation for the northern and coastal regions of Brazil, much of the central–southern Andes, and west of the Chaco jet exit region over Paraguay. Similarly, we find consistent

qualitative agreement between our findings and those of Nunez *et al.* (2009), Cabré *et al.* (2016), Falco *et al.* (2019), and Bozkurt *et al.* (2019) regarding changes in Chilean precipitation under a high emissions scenario (A2) or the RCP8.5 scenario. More specifically, drier (wetter) conditions in the south-central (southernmost) region of Chile in JJA and generally drier conditions throughout Chile during DJF.

Although some South American regions do not show a statistically significant change in precipitation (e.g., Chile), an increase in interannual variability, or more volatile precipitation characterized by “booms and busts”, is found. In addition, warming across the Andes leads to large reductions in snowpack and a near complete loss of the Tundra Köppen–Geiger climate, which is missed when coarser model projections of future climate are used (Beck *et al.*, 2018). Many of the hydroclimatic outcomes identified in this study such as elevation-dependent warming, increased winter-season precipitation volatility, and loss of snowpack are consistent with

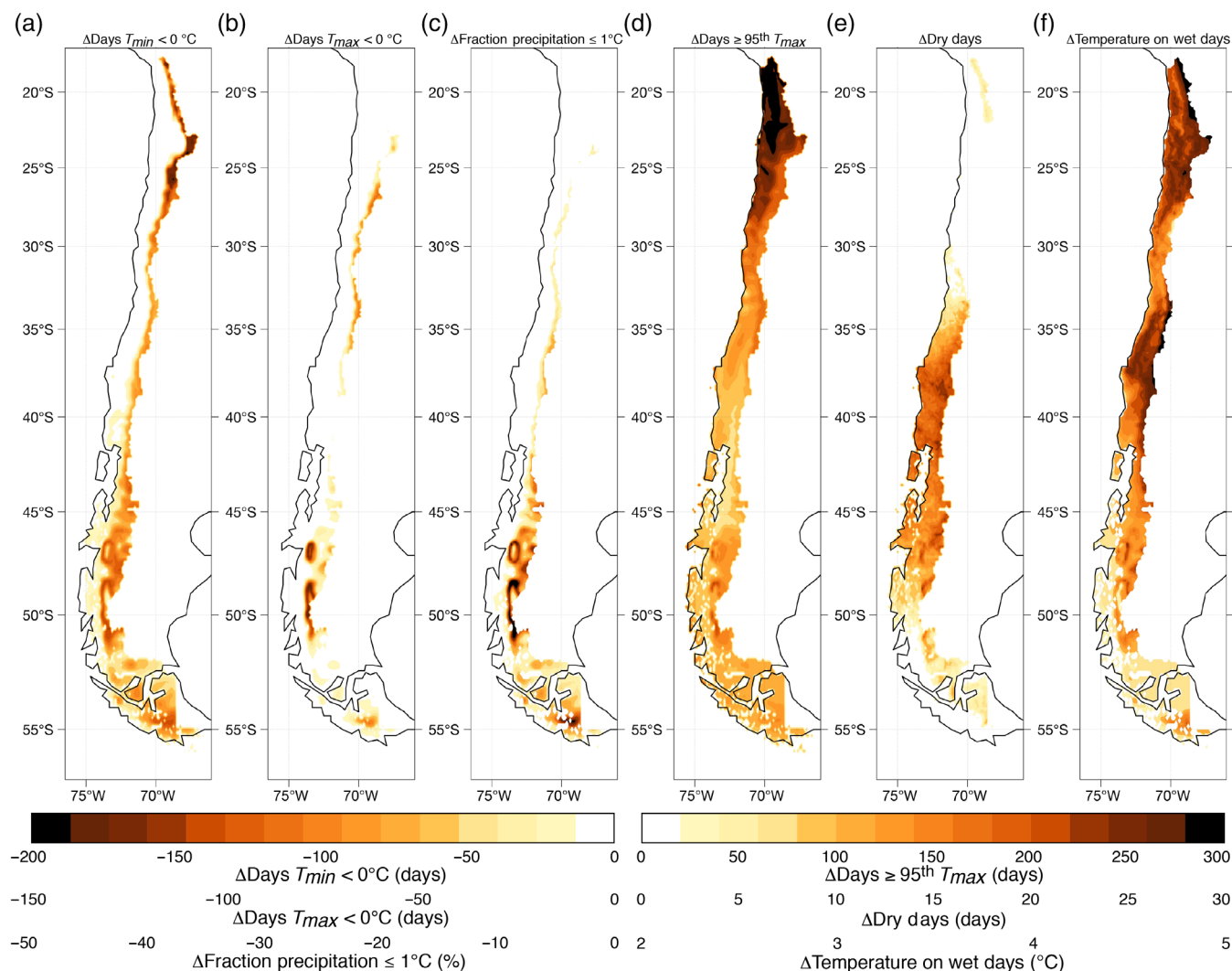


FIGURE 15 Differences between future (2070–2099; and historic (1985–2014) periods for the [Panel (a)] median annual number of days below freezing ($T_{max} \leq 0^\circ\text{C}$), [Panel (b)] change in fraction of cool season precipitation occur at or below $+1^\circ\text{C}$, [Panel (c)] change in T_{max} on wet days, [Panel (d)] change in the number of hot days ($T_{max} \geq 40^\circ\text{C}$), and [Panel (e)] change in the number of days exceeding the 95th percentile (parenthetical values in the colour bar)

climate change findings of other midlatitude mountain ranges (Rangwala and Miller, 2012; Pepin *et al.*, 2015; Huss *et al.*, 2017; Rhoades *et al.*, 2017; Beniston *et al.*, 2018; Swain *et al.*, 2018; Rhoades *et al.*, 2020b).

An important challenge for this model evaluation is related to the ability of reanalysis data sets to represent the observed precipitation and temperature reliably across regions of complex topography and limited number of observations (Condom *et al.*, 2020). One of the most alarming conclusions from multiple reanalysis evaluation studies is that we cannot completely trust data products that are often considered truth (Lundquist *et al.*, 2019), since statistical gridded products are not equivalent to actual observations. Schumacher *et al.* (2020) found that different reanalysis data sets vary significantly over the Chilean Andes, and the differences

are mostly attributed to spatial resolution and the number of observations used. Large discrepancies between products are also prevalent for precipitation estimates over arid regions due to the methodological challenges associated with the rare occurrence of precipitation events (Alvarez-Garreton *et al.*, 2018).

While our VR-Andes simulations are a major step forward in providing future climate projections over South America that can inform actionable climate adaptation strategies, they come with important limitations. These limitations stem from the fact that the VR-Andes simulations are a single-model, single 30-year member and only project one future climate scenario (all due to computational constraints). Nonetheless, our 30-year historical VR-Andes simulation shows comparable or better agreement with three reanalyses than previous modelling

studies (Solman, 2013; Solman *et al.*, 2013; Solman and Blázquez, 2019). However, we find that agreement is better in 2 m surface temperature than precipitation, with notable disagreement in the Andes during austral summer. These differences are undoubtedly influenced by the lack of long term, spatially complete in situ networks throughout the South American Andes Poveda *et al.* (2020), but may also be due to long-standing model biases. This includes: drizzle effects from sub-grid-scale parameterizations (e.g., too-often saturated model columns from the cumulus parameterization [Chen and Dai, 2018]), an long-standing erroneous double intertropical convergence zone (Wehner *et al.*, 2014), and non-convergence of mean and extreme precipitation with resolution refinement (Wehner *et al.*, 2014; Herrington and Reed, 2017; Chen and Dai, 2019; Herrington and Reed, 2020). That said, there are multiple lines of evidence showing that more refined model resolutions, particularly over mountainous and glaciated regions, enhance model veracity in CESM (Wehner *et al.*, 2014; Rhoades *et al.*, 2016, 2018; van Kampenhout *et al.*, 2019).

Last, our choice to use a static, high-resolution land-surface cover for all simulated periods may be unrealistic given expected land-use changes (e.g., deforestation and wildfires). The aforementioned limitations could all be addressed with more follow-up studies that assess VR-Andes sensitivities to horizontal resolution, the use of convective parameterizations, land-surface cover resolution and change, and/or future climate scenario.

Through our analysis of South American-wide climatic changes in temperature and precipitation, we identified several sub-regions within South America that warrant further study. These include: (a) the wet, dry, wet latitudinal pattern in Chile during austral winter; (b) the widespread increase in convective precipitation across the high-altitude Andes; (c) the drying of the northeastern portions of the Amazon in both austral winter and summer; and (d) the consistently wetter conditions in the region most influenced by the presence or absence of a Chaco jet (Ramos *et al.*, 2019) over the southeastern coastline of Brazil. Further, we identified “hot spots” of climatic change through the use of Köppen–Geiger climates that account for the interactions between temperature and precipitation. Major changes in historical Köppen–Geiger climates include the near Andes-wide elimination of the Tundra (or Alpine) climate, the desertification of western coastal regions of South America, and the large expansion of dry winter tropical savannah in the northeastern and central regions of South America.

One challenge with Köppen–Geiger climatological classifications, however, is that this approach does not explicitly account for changes in snow accumulation and

persistence, which is expected to undergo notable reductions (14). This, in addition to changes in the type, frequency, and magnitude of extreme weather and climate events, poses a limitation for estimating the true ecological impact of Köppen–Geiger climate changes. Therefore, these changes may be conservative estimates of climate change impacts on natural and human systems.

Although beyond the scope of this study, we plan to more robustly investigate the causal mechanisms of some of the aforementioned climate projections. For example, the expected changes in meridional precipitation distribution over Chile are hypothesized to result from shifts in atmospheric river activity and character, analogous to the western United States (Rhoades *et al.*, 2020b). Supporting this hypothesis is the finding that northern Chile does not experience an increase in the number of wet days, but precipitation (Figure 15) and peak SWE does increase (Figure 14). In the southern region of Chile, precipitation remains similar (or increases); however, an increase in the number of dry days is observed. In both cases, this would imply that precipitation days will become more extreme, which is consistent with recent trends of more frequent and severe extreme precipitation events in the Andes (Poveda *et al.*, 2020). By analysing changes in Chilean ARs we will implicitly identify shifts in midlatitude storm track and potentially explain the marked increase in the number of dry days in central Chile. This may also provide insight on the mechanisms that promote drought in this region and how drought regularity and persistence may shift due to climate change (Garreaud *et al.*, 2020).

The impacts of projected warming and drying in Central Chile in the VR-Andes simulations will be compounded by the near-complete elimination of the Chilean cryosphere by end-century if greenhouse gas emissions continue unabated. We hypothesize this decline results from an increase in the background temperature, specifically the number of days above 0°C, and a net warming of temperatures during precipitation events (Figure 15). The combined effect of warming and precipitation phase shifts (i.e., more rain and less snow) are likely the key contributors to the reduced quantity and earlier timing of water stored as snowpack. Alterations to precipitation phase is most pronounced over glaciated regions (Figure 15c,f). As such, we expect acceleration of glacial retreat as temperatures continue to rise (Figure 15a,d). These marked changes in the Chilean cryosphere have important implications on both water availability and natural hazard risk on downstream communities (Immerzeel *et al.*, 2020) as well as sea level rise (Dussailant *et al.*, 2018). This warrants a more fine-tuned analysis. Examples of future studies include an examination of changes in various snowpack properties in both

the accumulation and melt season across the Andean hypsometry, the implications of the snow-albedo feedback versus atmospheric moistening that shape elevation-dependent warming, and alterations to the

frequency of compound extremes (e.g., rain-on-snow and extreme precipitation on saturated soils and resultant landslide hazard). Given their unprecedented spatiotemporal resolution, VR-Andes simulations can also serve as

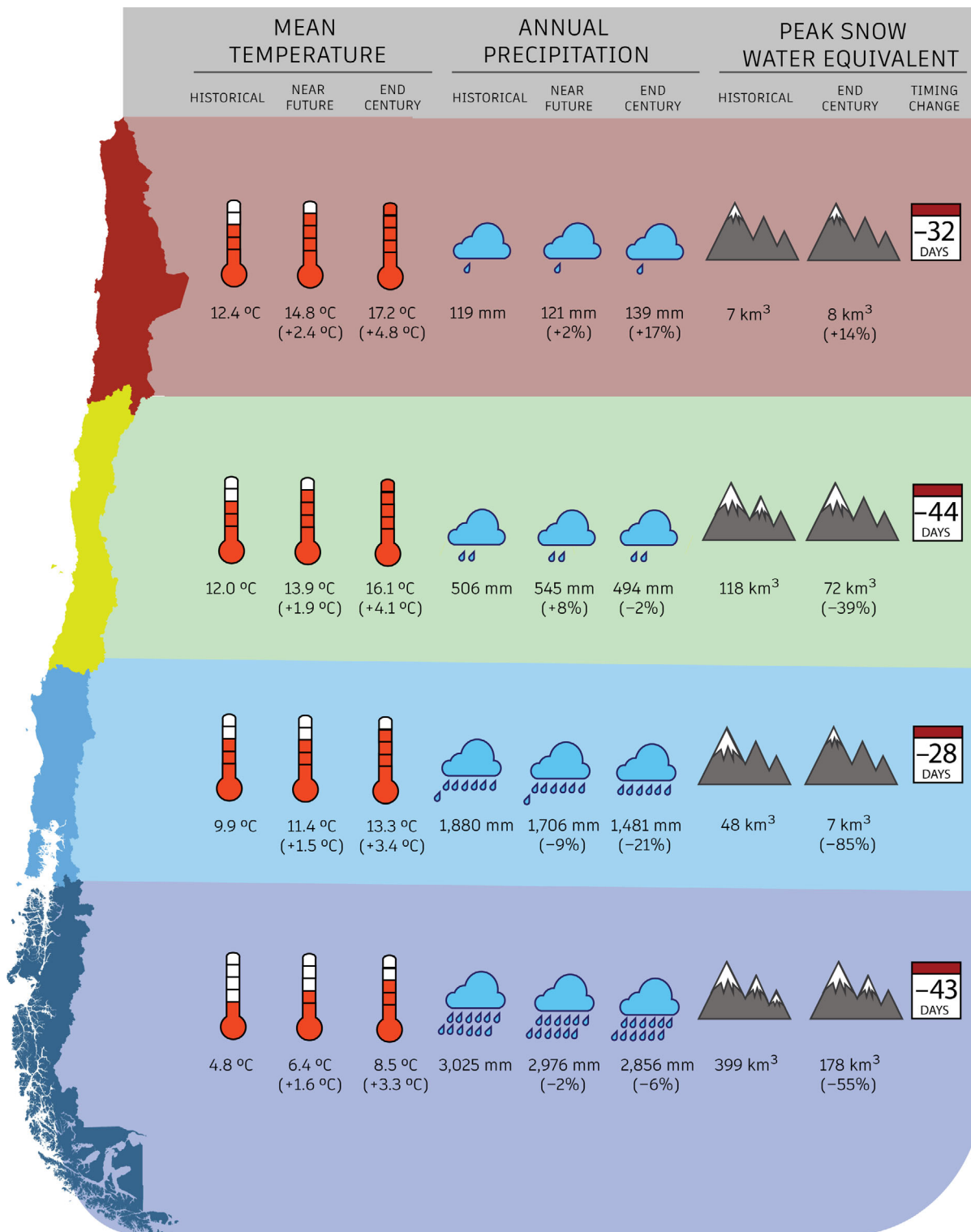


FIGURE 16 A summary of projected climate change impacts on mean temperature, mean annual precipitation, and median peak snow water equivalent and timing across four major regions of Chile

input to glaciological models enabling the examination of glacial mass loss and retreat. The various Chilean hydro-climatic changes shown in this study are summarized in Figure 16, which distil some key findings discussed throughout this study and aims to inform decision makers in need of climate change information (Briley *et al.*, 2020) over this region. Our findings are qualitatively consistent with previous work, however the more refined resolutions over the Andes provides additional evidence for the negative impacts of warming on society and ecosystems, especially when viewed through the lens of the loss of the Andean cryosphere and potential implications for water supply reliability. To better tailor these results to decision making, we anticipate additional evaluations of changes in other high elevation regions (e.g., Argentina, Bolivia, Ecuador, and Peru).

5 | CONCLUSIONS

Variable-resolution enabled Community Earth System Model simulations that telescope grid resolution from 111 km to 14 km over South America (defined as VR-Andes in this study) was done following the South American Coordinated Regional Downscaling Experiment domain specifications and the Atmosphere Model Intecomparison Project protocols. A primary goal was to produce high-resolution simulations over the topographically complex and climatically sensitive Andean mountains and provide a more detailed analysis of regional climatic change, namely in the Chilean Andes. Austral winter precipitations and temperatures and austral summer temperatures from the historical simulation (1985–2014) were found to compare well against commonly used reanalysis products at the continental scale, particularly when juxtaposed with previous modelling experiments. Notable biases were found in austral summer precipitation throughout much of the Andes, but may be partly due to the sparse in situ network. The VR-Andes simulations were also performed for two 30-year periods in the near future (2030–2059) and end-century (2070–2099) under the RCP8.5 scenario. We found a wide spread and significant warming across South America in both the near future and end-century, irregardless of season, and a more heterogeneous response in precipitation. Drastic climate changes emerged over certain South American regions including Chile, the northeastern Amazon, the eastern coast of Brazil, and the Andes, particularly when viewed through the lens of the Köppen–Geiger climate classification system. To provide a more granular analysis of one of these climate change “hot spots” we focused on Chile due to its meridional extent and reliance on Andean-derived water supply. The key regional changes for Chile are summarized as an

infographic in Figure 16. Qualitative comparisons with previous climate change projections over Chile are consistent with VR-Andes in both the sign and spatial location of change in DJF and JJA (Nunez *et al.*, 2009; Solman, 2013; Cabré *et al.*, 2016), yet are provided with more granularity in this study. Results indicate robust warming and spatially heterogeneous changes in precipitation variability and volatility. Earlier timing of peak snow water equivalent, warming of wet days, and fewer days below 0°C all are expected to drive a decline of Chile’s cryosphere.

Despite these stark projections, we do note that we only examine one future climate scenario, which corresponds to a world in which greenhouse gas emissions continue to rise unabated through the end of the century. If global effort to cut emissions is successful, we expect the simulated changes to be less severe for the end-century period. However, future climate scenarios typically differ less during near-future periods, so our mid-century results are likely to occur even if aggressive mitigation policies are pursued in the coming decades. Many open questions result from our analysis including how climate change influences the drivers, character, and prevalence of climatic extremes such as impactful atmospheric river events (Viale *et al.*, 2018), heat waves (Feron *et al.*, 2019), drought (Rodrigues *et al.*, 2019) and other wildfire-favouring conditions such as downslope windstorms (Abatzoglou *et al.*, 2020), glacial decline (Braun *et al.*, 2019), and flood events (Li *et al.*, 2020). Similarly, ecosystem responses to climate change including the identification of ecoregions that are most susceptible to or most resilient to change [e.g., ‘climate refugia’; (Ackerly *et al.*, 2020)] requires further investigation. Follow-up studies that examine these phenomena are planned and we welcome collaboration in this effort. We hope that the VR-Andes simulations will enable more granular assessments of projected climate change and help to build climate resiliency in South America.

ACKNOWLEDGEMENTS

Author Bambach was funded by Centro de Cambio Global at Pontifical Catholic University of Chile and the National Science Foundation award EF1137306/MIT sub-award 5710003122 to the University of California Davis. Author Rhoades was funded by the U.S. Department of Energy, Office of Biological and Environmental Research (DOE-BER) via the Regional and Global Climate Modelling Program (RGCM) through the “the Calibrated and Systematic Characterization, Attribution and Detection of Extremes (CASCADE)” Science Focus Area (award no. DE-AC02-05CH11231). Author Hatchett was supported by start-up funds provided by the Division of Atmospheric Science at the Desert Research Institute. Authors Jones, Rhoades, Ullrich, and Zarzycki

were funded by the DOE-BER RGCM funded project “An Integrated Evaluation of the Simulated Hydroclimate System of the Continental US” (award no. DE-SC0016605). We greatly appreciate the constructive suggestions provided by two reviewers and Associate Editor Jose Morengo. We would like to acknowledge high-performance computing support from Cheyenne (doi: 10.5065/D6RX99HX) provided by NCAR’s Computational and Information Systems Laboratory, sponsored by the National Science Foundation. Additionally, we would like to acknowledge that the simulations were analysed using resources of the National Energy Research Scientific Computing Center (NERSC), a U.S. Department of Energy Office of Science User Facility operated under Contract No. DE-AC02-05CH11231. The VR-Andes simulations generated for this study are accessible via a NERSC Science Gateway at the following URLs: https://portal.nersc.gov/archive/home/a/arhoades/Shared/www/atm/Chile_VR14_CAM5_4_CLM5_0; https://portal.nersc.gov/archive/home/a/arhoades/Shared/www/lnd/Chile_VR14_CAM5_4_CLM5_0; https://portal.nersc.gov/archive/home/a/arhoades/Shared/www/atm/Chile_VR14_CAM5_4_CLM5_0_RCP85; https://portal.nersc.gov/archive/home/a/arhoades/Shared/www/lnd/Chile_VR14_CAM5_4_CLM5_0_RCP85.

AUTHOR CONTRIBUTIONS

Nicolas Bambach: Conceptualization; formal analysis; funding acquisition; investigation; methodology; visualization; writing – original draft; writing – review and editing. **Alan Rhoades:** Conceptualization; data curation; formal analysis; funding acquisition; investigation; methodology; software; visualization; writing – original draft; writing – review and editing. **Benjamin Hatchett:** Formal analysis; investigation; visualization; writing – original draft; writing – review and editing. **Andrew D. Jones:** Resources; supervision. **Paul Ullrich:** Conceptualization; funding acquisition; methodology; resources; software; supervision; writing – review and editing. **Colin Zarzycki:** Methodology; software; writing – review and editing.

ORCID

Nicolas E. Bambach  <https://orcid.org/0000-0002-5060-8781>

Alan M. Rhoades  <https://orcid.org/0000-0003-3723-2422>

Benjamin J. Hatchett  <https://orcid.org/0000-0003-1066-3601>

REFERENCES

Abatzoglou, J.T., Hatchett, B.J., Fox-Hughes, P., Gershunov, A. and Nauslar, N.J. (2020) Global climatology of synoptically-forced

downslope winds. *International Journal of Climatology*, 41(1), 31–50. <https://doi.org/10.1002/joc.6607>.

- Ackerly, D.D., Kling, M.M., Clark, M.L., Papper, P., Oldfather, M. F., Flint, A.L. and Flint, L.E. (2020) Topoclimates, refugia, and biotic responses to climate change. *Frontiers in Ecology and the Environment*, 18(5), 288–297. <https://doi.org/10.1002/fee.2204>.
- Adam, O., Schneider, T. and Brient, F. (2018) Regional and seasonal variations of the double-itsz bias in cmip5 models. *Climate Dynamics*, 51(1), 101–117. <https://doi.org/10.1007/s00382-017-3909-1>.
- Alvarez-Garreton, C., Mendoza, P.A., Boisier, J.P., Addor, N., Galleguillos, M., Zambrano-Bigiarini, M., Lara, A., Puelma, C., Cortes, G., Garreaud, R., McPhee, J. and Ayala, A. (2018) The camels-cl dataset: catchment attributes and meteorology for large sample studies – Chile dataset. *Hydrology and Earth System Sciences*, 22(11), 5817–5846. <https://doi.org/10.5194/hess-22-5817-2018>. Available at: <https://hess.copernicus.org/articles/22/5817/2018/>.
- Andreoli, A., Mao, L., Iroume, A., Arumi, J.L., Nardini, A., Pizarro, R., Caamano, D., Meier, C. and Link, O. (2012) The need for a hydromorphological approach to Chilean river management. *Revista Chilena de Historia Natural*, 85(3), 339–343. Available at: <https://www.redalyc.org/articulo.oa?id=369944302008>.
- Arakawa, A. and Jung, J.-H. (2011) Multiscale modeling of the moist-convective atmosphere – a review. *Atmospheric Research*, 102(3), 263–285. <https://doi.org/10.1016/j.atmosres.2011.08.009>.
- Ávila, Á., Guerrero, F.C., Escobar, Y.C. and Justino, F. (2019) Recent precipitation trends and floods in the colombian Andes. *Water*, 11(2), 379. <https://doi.org/10.3390/w11020379>.
- Beck, H.E., Zimmermann, N.E., McVicar, T.R., Vergopolan, N., Berg, A. and Wood, E.F. (2018) Present and future Köppen-Geiger climate classification maps at 1-km resolution. *Scientific data*, 5, 180214. <https://doi.org/10.1038/sdata.2018.214>.
- Beniston, M., Farinotti, D., Stoffel, M., Andreassen, L.M., Coppola, E., Eckert, N., Fantini, A., Giacomini, F., Hauck, C., Huss, M., Huwald, H., Lehning, M., López-Moreno, J.-I., Magnusson, J., Marty, C., Morán-Tejeda, E., Morin, S., Naaim, M., Provenzale, A., Rabatel, A., Six, D., Stötter, J., Strasser, U., Terzago, S. and Vincent, C. (2018) The European mountain cryosphere: a review of its current state, trends, and future challenges. *The Cryosphere*, 12(2), 759–794. <https://doi.org/10.5194/tc-12-759-2018>.
- Benjamini, Y. and Hochberg, Y. (1995) Controlling the false discovery rate: a practical and powerful approach to multiple testing. *Journal of the Royal Statistical Society. Series B (Methodological)*, 57(1), 289–300. Available at: <http://www.jstor.org/stable/2346101>.
- Boisier, J.P., Alvarez-Garreton, C., Cordero, R.R., Damiani, A., Gallardo, L., Garreaud, R.D., Lambert, F., Ramallo, C., Rojas, M. and Rondanelli, R. (2018) Anthropogenic drying in central-southern Chile evidenced by long-term observations and climate model simulations. *Elementa: Science of the Anthropocene*, 6, 74. <https://doi.org/10.1525/elementa.328>.
- Boulanger, J.-P., Brasseur, G., Carril, A.F., de Castro, M., Degallier, N., Ereño, C., Le Treut, H., Marengo, J.A., Menendez, C.G., Nuñez, M.N., Penalba, O.C., Rolla, A.L., Rusticucci, M. and Terra, R. (2010) A Europe–south America network for climate change assessment and impact studies. *Climatic Change*, 98(3), 307–329. <https://doi.org/10.1007/s10584-009-9734-8>.

- Bowman, D.M., Moreira-Muñoz, A., Kolden, C.A., Chávez, R.O., Muñoz, A.A., Salinas, F., González-Reyes, Á., Rocco, R., de la Barrera, F., Williamson, G.J., Borchers, N., Cifuentes, L.A., Abatzoglou, J.T. and Johnston, F.H. (2019) Human-environmental drivers and impacts of the globally extreme 2017 Chilean fires. *Ambio*, 48(4), 350–362.
- Bozkurt, D., Rojas, M., Boisier, J.P., Rondanelli, R., Garreaud, R. and Gallardo, L. (2019) Dynamical downscaling over the complex terrain of Southwest South America: present climate conditions and added value analysis. *Climate Dynamics*, 53(11), 6745–6767. <https://doi.org/10.1007/s00382-019-04959-y>.
- Bozkurt, D., Rondanelli, R., Garreaud, R. and Arriagada, A. (2016) Impact of warmer eastern tropical Pacific SST on the March 2015 Atacama floods. *Monthly Weather Review*, 144(11), 4441–4460.
- Braun, M.H., Malz, P., Sommer, C., Fariás-Barahona, D., Sauter, T., Casassa, G., Soruco, A., Skvarca, P. and Seehaus, T.C. (2019) Constraining glacier elevation and mass changes in South America. *Nature Climate Change*, 9(2), 130–136. <https://doi.org/10.1038/s41558-018-0375-7>.
- Briley, L., Kelly, R., Blackmer, E.D., Troncoso, A.V., Rood, R.B., Andresen, J. and Lemos, M.C. (2020) Increasing the usability of climate models through the use of consumer-report-style resources for decision-making. *Bulletin of the American Meteorological Society*, 101(10), E1709–E1717. <https://doi.org/10.1175/BAMS-D-19-0099.1>.
- Cabré, M.F., Solman, S. and Núñez, M. (2016) Regional climate change scenarios over southern South America for future climate (2080–2099) using the mm5 model. Mean, interannual variability and uncertainties. *Atmosfera*, 29(1), 35–60. <https://doi.org/10.20937/ATM.2016.29.01.04>.
- Chen, D. and Chen, H.W. (2013) Using the Köppen classification to quantify climate variation and change: an example for 1901–2010. *Environmental Development*, 6, 69–79. <https://doi.org/10.1016/j.envdev.2013.03.007>.
- Chen, D. and Dai, A. (2018) Dependence of estimated precipitation frequency and intensity on data resolution. *Climate Dynamics*, 50(9–10), 3625–3647. <https://doi.org/10.1007/s00382-017-3830-7>.
- Chen, D. and Dai, A. (2019) Precipitation characteristics in the community atmosphere model and their dependence on model physics and resolution. *Journal of Advances in Modeling Earth Systems*, 11(7), 2352–2374. <https://doi.org/10.1029/2018MS001536>.
- Chou, S.C., Nunes, A.M.B. and Cavalcanti, I.F.A. (2000) Extended range forecasts over South America using the regional eta model. *Journal of Geophysical Research: Atmospheres*, 105(D8), 10147–10160. <https://doi.org/10.1029/1999JD901137>.
- Collier, N., Hoffman, F.M., Lawrence, D.M., Keppel-Aleks, G., Koven, C.D., Riley, W.J., Mu, M. and Randerson, J.T. (2018) The international land model benchmarking (ILAMB) system: design, theory, and implementation. *Journal of Advances in Modeling Earth Systems*, 10(11), 2731–2754. <https://doi.org/10.1029/2018MS001354>.
- Condom, T., Martínez, R., Pabón, J.D., Costa, F., Pineda, L., Nieto, J.J., López, F. and Villacis, M. (2020) Climatological and hydrological observations for the South American Andes: in situ stations, satellite, and reanalysis data sets. *Frontiers in Earth Science*, 8, 92. <https://doi.org/10.3389/feart.2020.00092>.
- Danabasoglu, G., Lamarque, J.-F., Bacmeister, J., Bailey, D.A., DuVivier, A.K., Edwards, J., Emmons, L.K., Fasullo, J., Garcia, R., Gettelman, A., Hannay, C., Holland, M.M., Large, W.G., Lauritzen, P.H., Lawrence, D.M., Lenaerts, J.T.M., Lindsay, K., Lipscomb, W.H., Mills, M.J., Neale, R., Oleson, K.W., Otto-Bliesner, B., Phillips, A.S., Sacks, W., Tilmes, S., van Kampenhou, L., Vertenstein, M., Bertini, A., Dennis, J., Deser, C., Fischer, C., Fox-Kemper, B., Kay, J.E., Kinnison, D., Kushner, P.J., Larson, V.E., Long, M.C., Mickelson, S., Moore, J.K., Nienhouse, E., Polvani, L., Rasch, P.J. and Strand, W.G. (2020) The community earth system model version 2 (CESM2). *Journal of Advances in Modeling Earth Systems*, 12(2), e2019MS001916. <https://doi.org/10.1029/2019MS001916>.
- Díaz, L.B., Saurral, R.I. and Vera, C.S. (2021) Assessment of South America summer rainfall climatology and trends in a set of global climate models large ensembles. *International Journal of Climatology*, 41, E59–E77. <https://doi.org/10.1002/joc.6643>.
- Dussailant, I., Berthier, E. and Brun, F. (2018) Geodetic mass balance of the northern Patagonian icefield from 2000 to 2012 using two independent methods. *Frontiers in Earth Science*, 6, 8.
- Espinoza, J.C., Garreaud, R., Poveda, G., Arias, P.A., Molina-Carpio, J., Masiokas, M., Viale, M. and Scaff, L. (2020) Hydroclimate of the Andes part I: Main climatic features. *Frontiers in Earth Science*, 8, 64. <https://doi.org/10.3389/feart.2020.00064>.
- Falco, M., Carril, A.F., Menéndez, C.G., Zaninelli, P.G. and Li, L.Z. X. (2019) Assessment of CORDEX simulations over South America: added value on seasonal climatology and resolution considerations. *Climate Dynamics*, 52, 4771–4786. <https://doi.org/10.1007/s00382-018-4412-z>.
- FAO. (2012) *Diagnostico Nacional de Montaña*. Food and Agriculture Organization of the United Nations: Informe Chile.
- Ferguson, J.O., Jablonowski, C., Johansen, H., McCorquodale, P., Colella, P. and Ullrich, P.A. (2016) Analyzing the adaptive mesh refinement (AMR) characteristics of a high-order 2D cubed-sphere shallow-water model. *Monthly Weather Review*, 144(12), 4641–4666. <https://doi.org/10.1175/MWR-D-16-0197.1>.
- Feron, S., Cordero, R.R., Damiani, A., Llanillo, P., Jorquera, J., Sepulveda, E., Asencio, V., Laroze, D., Labbe, F., Carrasco, J. and Torres, G. (2019) Observations and projections of heat waves in South America. *Scientific Reports*, 9(1), 1–15. <https://doi.org/10.1038/s41598-019-44614-4>.
- Field, C.B. (2014) *Climate Change 2014—Impacts, Adaptation and Vulnerability: Regional Aspects*. New York: Cambridge University Press.
- Fonseca, M.G., Alves, L.M., Aguiar, A.P.D., Arai, E., Anderson, L.O., Rosan, T.M., Shimabukuro, Y.E. and de Aragão, L.E.O.E.C. (2019) Effects of climate and land-use change scenarios on fire probability during the 21st century in the Brazilian Amazon. *Global Change Biology*, 25(9), 2931–2946. <https://doi.org/10.1111/gcb.14709>.
- Funk, C., Peterson, P., Landsfeld, M., Pedreros, D., Verdin, J., Shukla, S., Husak, G., Rowland, J., Harrison, L., Hoell, A. and Michaelsen, J. (2015) The climate hazards infrared precipitation with stations—a new environmental record for monitoring extremes. *Scientific Data*, 2(1), 1–21. <https://doi.org/10.1038/sdata.2015.66>.

- Garreaud, R.D., Alvarez-Garreton, C., Barichivich, J., Boisier, J.P., Christie, D., Galleguillos, M., LeQuesne, C., McPhee, J. and Zambrano-Bigiarini, M. (2017) The 2010–2015 megadrought in Central Chile: impacts on regional hydroclimate and vegetation. *Hydrology & Earth System Sciences*, 21(12), 6307–6327. <https://doi.org/10.5194/hess-2017-191>.
- Garreaud, R.D., Boisier, J.P., Rondanelli, R., Montecinos, A., Sepúlveda, H.H. and Veloso-Aguila, D. (2020) The Central Chile mega drought (2010–2018): a climate dynamics perspective. *International Journal of Climatology*, 40(1), 421–439.
- Garreaud, R.D., Molina, A. and Farias, M. (2010) Andean uplift, ocean cooling and Atacama hyperaridity: a climate modeling perspective. *Earth and Planetary Science Letters*, 292(1), 39–50. <https://doi.org/10.1016/j.epsl.2010.01.017>.
- Gates, W.L., Boyle, J.S., Covey, C., Dease, C.G., Doutriaux, C. M., Drach, R.S., Fiorino, M., Gleckler, P.J., Hnilo, J.J., Marlais, S.M., Phillips, T.J., Potter, G.L., Santer, B.D., Sperber, K.R., Taylor, K.E. and Williams, D.N. (1999) An overview of the results of the atmospheric model Intercomparison project (AMIP I). *Bulletin of the American Meteorological Society*, 80(1), 29–56. [https://doi.org/10.1175/1520-0477\(1999\)080<0029:A00TRO>2.0.CO;2](https://doi.org/10.1175/1520-0477(1999)080<0029:A00TRO>2.0.CO;2).
- Gelaro, R., McCarty, W., Suárez, M.J., Todling, R., Molod, A., Takacs, L., Randles, C.A., Darmenov, A., Bosilovich, M.G., Reichle, R., Wargan, K., Coy, L., Cullather, R., Draper, C., Akella, S., Buchard, V., Conaty, A., da Silva, A.M., Gu, W., Kim, G.-K., Koster, R., Lucchesi, R., Merkova, D., Nielsen, J.E., Partyka, G., Pawson, S., Putman, W., Rienecker, M., Schubert, S.D., Sienkiewicz, M. and Zhao, B. (2017) The modern-era retrospective analysis for research and applications, version 2 (MERRA-2). *Journal of Climate*, 30(14), 5419–5454. <https://doi.org/10.1175/JCLI-D-16-0758.1>.
- Gottelman, A., Callaghan, P., Larson, V.E., Zarzycki, C.M., Bacmeister, J., Lauritzen, P.H., Bogenschutz, P.A. and Neale, R. (2018) Regional climate simulations with the Community Earth System Model. *Journal of Advances in Modeling Earth Systems*, 10(6), 1245–1265. <https://doi.org/10.1002/2017MS001227>.
- Gottelman, A. and Morrison, H. (2015) Advanced two-moment bulk microphysics for global models. Part I: off-line tests and comparison with other schemes. *Journal of Climate*, 28(3), 1268–1287. <https://doi.org/10.1175/JCLI-D-14-00102.1>.
- Gottelman, A., Morrison, H., Santos, S., Bogenschutz, P. and Caldwell, P.M. (2015) Advanced two-moment bulk microphysics for global models. Part II: global model solutions and aerosol–cloud interactions. *Journal of Climate*, 28(3), 1288–1307. <https://doi.org/10.1175/JCLI-D-14-00103.1>.
- Giorgi, F. (2019) Thirty years of regional climate modeling: where are we and where are we going next? *Journal of Geophysical Research: Atmospheres*, 124(11), 5696–5723. <https://doi.org/10.1029/2018JD030094>.
- Gómez-González, S., González, M.E., Paula, S., Díaz-Hormazábal, I., Lara, A. and Delgado-Baquerizo, M. (2019) Temperature and agriculture are largely associated with fire activity in Central Chile across different temporal periods. *Forest Ecology and Management*, 433, 535–543.
- Gutowski, W.J., Ullrich, P.A., Hall, A., Leung, L.R., O'Brien, T.A., Patricola, C.M., Arritt, R.W., Bukovsky, M.S., Calvin, K.V., Feng, Z., Jones, A.D., Kooperman, G.J., Monier, E., Pritchard, M.S., Pryor, S.C., Qian, Y., Rhoades, A.M., Roberts, A.F., Sakaguchi, K., Urban, N. and Zarzycki, C. (2020) The ongoing need for high-resolution regional climate models: process understanding and stakeholder information. *Bulletin of the American Meteorological Society*, 101(5), E664–E683. <https://doi.org/10.1175/BAMS-D-19-0113.1>.
- Hamed, K.H. and Ramachandra Rao, A. (1998) A modified mann-kendall trend test for autocorrelated data. *Journal of Hydrology*, 204(1), 182–196. [https://doi.org/10.1016/S0022-1694\(97\)00125-X](https://doi.org/10.1016/S0022-1694(97)00125-X).
- Harris, L.M. and Lin, S.-J. (2013) A two-way nested global-regional dynamical core on the cubed-sphere grid. *Monthly Weather Review*, 141(1), 283–306. <https://doi.org/10.1175/MWR-D-11-00201.1>.
- Herrington, A.R. and Reed, K.A. (2017) An explanation for the sensitivity of the mean state of the community atmosphere model to horizontal resolution on aquaplanets. *Journal of Climate*, 30(13), 4781–4797. <https://doi.org/10.1175/JCLI-D-16-0069.1>.
- Herrington, A.R. and Reed, K.A. (2020) On resolution sensitivity in the community atmosphere model. *Quarterly Journal of the Royal Meteorological Society*, 146(733), 3789–3807. <https://doi.org/10.1002/qj.3873>.
- Huang, X., Rhoades, A.M., Ullrich, P.A. and Zarzycki, C.M. (2016) An evaluation of the variable-resolution CESM for modeling California's climate. *Journal of Advances in Modeling Earth Systems*, 8(1), 345–369. <https://doi.org/10.1002/2015MS000559>.
- Huang, X. and Ullrich, P.A. (2016) Irrigation impacts on California's climate with the variable-resolution CESM. *Journal of Advances in Modeling Earth Systems*, 8(3), 1151–1163. <https://doi.org/10.1002/2016MS000656>.
- Huang, X. and Ullrich, P.A. (2017) The changing character of 21st century precipitation over the western United States in the variable-resolution CESM. *Journal of Climate*, 30(18), 7555–7575. <https://doi.org/10.1175/JCLI-D-16-0673.1>.
- Huggel, C., Carey, M., Emmer, A., Frey, H., Walker-Crawford, N. and Wallimann-Helmer, I. (2020) Anthropogenic climate change and glacier lake outburst flood risk: local and global drivers and responsibilities for the case of lake palcacocha, Peru. *Natural Hazards and Earth System Sciences*, 20(8), 2175–2193. <https://doi.org/10.5194/nhess-20-2175-2020>.
- Huss, M., Bookhagen, B., Huggel, C., Jacobsen, D., Bradley, R., Clague, J., Vuille, M., Buytaert, W., Cayan, D., Greenwood, G., Mark, B., Milner, A., Weingartner, R. and Winder, M. (2017) Toward mountains without permanent snow and ice. *Earth's Future*, 5(5), 418–435. <https://doi.org/10.1002/2016EF000514>.
- Immerzeel, W.W., Lutz, A.F., Andrade, M., Bahl, A., Biemans, H., Bolch, T., Hyde, S., Brumby, S., Davies, B.J., Elmore, A.C., Emmer, A., Feng, M., Fernández, A., Haritashya, U., Kargel, J. S., Koppes, M., Kraaijenbrink, P.D., Kulkarni, A.V., Mayewski, P.A., Nepal, S., Pacheco, P., Painter, T.H., Pellicciotti, F., Rajaram, H., Rupper, S., Sinisalo, A., Shrestha, A.B., Viviroli, D., Wada, Y., Xiao, C., Yao, T. and Baillie, J.E. (2020) Importance and vulnerability of the world's water towers. *Nature*, 577(7790), 364–369. <https://doi.org/10.1038/s41586-019-1822-y>.
- Jennings, K., Winchell, T.S., Livneh, B. and Molotch, N.P. (2018) Spatial variation of the rain–snow temperature threshold across the northern hemisphere. *Nature Communications*, 9(1), 1–9. <https://doi.org/10.1038/s41467-018-03629-7>.

- Koeppen, W. (2011) The thermal zones of the earth according to the duration of hot, moderate and cold periods and to the impact of heat on the organic world. *Meteorologische Zeitschrift*, 20(3), 351–360. <https://doi.org/10.1127/0941-2948/2011/105>.
- Köppen, W. and Geiger, R. (1954) *Klima der erde (Climate of the Earth) Wall Map*. Gotha: Klett-Perthes.
- Kottek, M., Grieser, J., Beck, C., Rudolf, B. and Rubel, F. (2006) World map of the Köppen-Geiger climate classification updated. *Meteorologische Zeitschrift*, 15(3), 259–263. <https://doi.org/10.1127/0941-2948/2006/0130>.
- Lawrence, D.M., Fisher, R.A., Koven, C.D., Oleson, K.W., Swenson, S.C., Bonan, G., Collier, N., Ghimire, B., van Kampenhou, L., Kennedy, D., Kluzek, E., Lawrence, P.J., Li, F., Li, H., Lombardozzi, D., Riley, W.J., Sacks, W.J., Shi, M., Vertenstein, M., Wieder, W.R., Xu, C., Ali, A.A., Badger, A.M., Bisht, G., van den Broeke, M., Brunke, M.A., Burns, S.P., Buzan, J., Clark, M., Craig, A., Dahlin, K., Drewniak, B., Fisher, J.B., Flanner, M., Fox, A.M., Gentine, P., Hoffman, F., Keppel-Aleks, G., Knox, R., Kumar, S., Lenaerts, J., Leung, L.R., Lipscomb, W.H., Lu, Y., Pandey, A., Pelletier, J.D., Perket, J., Randerson, J.T., Ricciuto, D.M., Sanderson, B.M., Slater, A., Subin, Z.M., Tang, J., Thomas, R.Q., Val Martin, M. and Zeng, X. (2019) The community land model version 5: description of new features, benchmarking, and impact of forcing uncertainty. *Journal of Advances in Modeling Earth Systems*, 11(12), 4245–4287. <https://doi.org/10.1029/2018MS001583>.
- Li, S., Otto, F.E.L., Harrington, L.J., Sparrow, S.N. and Wallom, D.C.H. (2020) A pan-south-america assessment of avoided exposure to dangerous extreme precipitation by limiting to 1.5°C warming. *Environmental Research Letters*, 15(5), 54005. <https://doi.org/10.1088/1748-9326/ab50a2>.
- Lundquist, J., Hughes, M., Gutmann, E. and Kapnick, S. (2019) Our skill in modeling mountain rain and snow is bypassing the skill of our observational networks. *Bulletin of the American Meteorological Society*, 100(12), 2473–2490. <https://doi.org/10.1175/BAMS-D-19-0001.1>. Available at: <https://journals.ametsoc.org/view/journals/bams/100/12/bams-d-19-0001.1.xml>.
- Marengo, J.A., Ambrizzi, T., Da Rocha, R.P., Alves, L.M., Cuadra, S.V., Valverde, M.C., Torres, R.R., Santos, D.C. and Ferraz, S.E. (2010) Future change of climate in south america in the late twenty-first century: intercomparison of scenarios from three regional climate models. *Climate Dynamics*, 35(6), 1073–1097.
- Marengo, J.A., Chou, S.C., Kay, G., Alves, L.M., Pesquero, J.F., Soares, W.R., Santos, D.C., Lyra, A.A., Sueiro, G., Betts, R., Chagas, D.J., Gomes, J.L., Bustamante, J.F. and Tavares, P. (2012) Development of regional future climate change scenarios in south america using the eta cptec/hadcm3 climate change projections: climatology and regional analyses for the amazon, são francisco and the paraná river basins. *Climate Dynamics*, 38(9–10), 1829–1848.
- Masiokas, M., Rabatel, A., Rivera Ibáñez, A., Ruiz, L., Pitte, P., Ceballos, J.L., Barcaza, G., Soruco, A., Bown, F., Berthier, E., Dussailant, I. and MacDonell, S. (2020) A review of the current state and recent changes of the andean cryosphere. *Frontiers in Earth Science*, 8, 99. <https://doi.org/10.3389/feart.2020.00099>.
- Menne, M.J., Durre, I., Vose, R.S., Gleason, B.E. and Houston, T.G. (2012) An overview of the global historical climatology network-daily database. *Journal of Atmospheric and Oceanic Technology*, 29(7), 897–910. <https://doi.org/10.1175/JTECH-D-11-00103.1>.
- Naumann, G., Vargas, W.M., Barbosa, P., Blauhut, V., Spinoni, J. and Vogt, J.V. (2019) Dynamics of socioeconomic exposure, vulnerability and impacts of recent droughts in Argentina. *Geosciences*, 9(1), 39. <https://doi.org/10.3390/geosciences9010039>.
- Nunez, M.N., Solman, S.A. and Cabré, M.F. (2009) Regional climate change experiments over southern South America. II: climate change scenarios in the late twenty-first century. *Climate Dynamics*, 32(7–8), 1081–1095. <https://doi.org/10.1007/s00382-008-0449-8>.
- Ochoa-Tocachi, B.F., Buytaert, W., Antiporta, J., Acosta, L., Bardales, J.D., Célleri, R., Crespo, P., Fuentes, P., Gil-Ríos, J., Guallpa, M., Llerena, C., Olaya, D., Pardo, P., Rojas, G., Villacís, M., Villazón, M., Viñas, P. and De Bièvre, B. (2018) High-resolution hydrometeorological data from a network of headwater catchments in the tropical Andes. *Scientific data*, 5, 180080. <https://doi.org/10.1038/sdata.2018.80>.
- Pabón-Caicedo, J.D., Arias, P.A., Carril, A.F., Espinoza, J.C., Borrel, L.F., Goubanova, K., Lavado-Casimiro, W., Masiokas, M., Solman, S. and Villalba, R. (2020) Observed and projected hydroclimate changes in the Andes. *Frontiers in Earth Science*, 8, 61. <https://doi.org/10.3389/feart.2020.00061>.
- Penalba, O., Rivera, J. and Pántano, V. (2014) The claris lpb database: constructing a long-term daily hydro-meteorological dataset for la Plata basin, southern south america. *Geoscience Data Journal*, 1, 20–29. <https://doi.org/10.1002/gdj3.7>.
- Pepin, N., Bradley, R.S., Diaz, H., Baraër, M., Caceres, E., Forsythe, N., Fowler, H., Greenwood, G., Hashmi, M., Liu, X., Miller, J.R., Liang, N., Ohmura, A., Palazzi, E., Rangwala, I., Schöner, W., Severskiy, I., Shahgedanova, M., Wang, M.B., Williamson, S.N. and Daqing, Y. (2015) Elevation-dependent warming in mountain regions of the world. *Nature Climate Change*, 5(5), 424–430. <https://doi.org/10.1038/nclimate2563>.
- Poveda, G., Espinoza, J.C., Zuluaga, M.D., Solman, S.A., Garreaud Salazar, R. and van Oevelen, P.J. (2020) High impact weather events in the Andes. *Frontiers in Earth Science*, 8, 162. <https://doi.org/10.3389/feart.2020.00162>.
- Ramos, A.M., Blamey, R.C., Algarra, I., Nieto, R., Gimeno, L., Tomé, R., Reason, C.J. and Trigo, R.M. (2019) From Amazonia to southern Africa: atmospheric moisture transport through low-level jets and atmospheric rivers. *Annals of the New York Academy of Sciences*, 1436(1), 217–230. <https://doi.org/10.1111/nyas.13960>.
- Rangwala, I. and Miller, J.R. (2012) Climate change in mountains: a review of elevation-dependent warming and its possible causes. *Climatic Change*, 114(3–4), 527–547. <https://doi.org/10.1007/s10584-012-0419-3>.
- Rauscher, S.A. and Ringler, T.D. (2014) Impact of variable-resolution meshes on Midlatitude Baroclinic eddies using CAM-MPAS-A. *Monthly Weather Review*, 142(11), 4256–4268. <https://doi.org/10.1175/MWR-D-13-00366.1>.
- Rhoades, A.M., Huang, X., Ullrich, P.A. and Zarzycki, C.M. (2016) Characterizing Sierra Nevada snowpack using variable-resolution CESM. *Journal of Applied Meteorology and Climatology*, 55(1), 173–196. <https://doi.org/10.1175/JAMC-D-15-0156.1>.
- Rhoades, A.M., Jones, A.D., O'Brien, T.A., O'Brien, J.P., Ullrich, P.A. and Zarzycki, C.M. (2020a) Influences of North Pacific

- Ocean domain extent on the Western U.S. Winter Hydroclimatology in variable-resolution CESM. *Journal of Geophysical Research: Atmospheres*, 125(14), e2019JD031977. <https://doi.org/10.1029/2019JD031977>.
- Rhoades, A.M., Jones, A.D., Srivastava, A., Huang, H., O'Brien, T.A., Patricola, C.M., Ullrich, P.A., Wehner, M.A. and Zhou, Y. (2020b) The shifting scales of Western US Landfalling atmospheric rivers under climate change. *Geophysical Research Letters*, 47(17), e2020GL089096. <https://doi.org/10.1029/2020GL089096>.
- Rhoades, A.M., Ullrich, P.A. and Zarzycki, C.M. (2017) Projecting 21st century snowpack trends in Western USA Mountains using variable-resolution CESM. *Climate Dynamics*, 50(1), 261–288. <https://doi.org/10.1007/s00382-017-3606-0>.
- Rhoades, A.M., Ullrich, P.A., Zarzycki, C.M., Johansen, H., Margulis, S.A., Morrison, H., Xu, Z. and Collins, W. (2018) Sensitivity of mountain hydroclimate simulations in variable-resolution cesm to microphysics and horizontal resolution. *Journal of Advances in Modeling Earth Systems*, 10(6), 1357–1380. <https://doi.org/10.1029/2018MS001326>.
- Riahi, K., Rao, S., Krey, V., Cho, C., Chirkov, V., Fischer, G., Kindermann, G., Nakicenovic, N. and Rafaj, P. (2011) RCP 8.5—a scenario of comparatively high greenhouse gas emissions. *Climatic Change*, 109(1), 33. <https://doi.org/10.1007/s10584-011-0149-y>.
- Rodrigues, J.A., Viola, M.R., Alvarenga, L.A., de Mello, C.R., Chou, S.C., de Oliveira, V.A., Uddameri, V. and Morais, M.A. (2020) Climate change impacts under representative concentration pathway scenarios on streamflow and droughts of basins in the brazilian cerrado biome. *International Journal of Climatology*, 40(5), 2511–2526. <https://doi.org/10.1002/joc.6347>.
- Rodrigues, R.R., Taschetto, A.S., Sen Gupta, A. and Foltz, G.R. (2019) Common cause for severe droughts in South America and marine heatwaves in the South Atlantic. *Nature Geoscience*, 12(8), 620–626. <https://doi.org/10.1038/s41561-019-0393-8>.
- Rondanelli, R., Hatchett, B., Rutilant, J., Bozkurt, D. and Garreaud, R. (2019) Strongest mjo on record triggers extreme Atacama rainfall and warmth in Antarctica. *Geophysical Research Letters*, 46(6), 3482–3491. <https://doi.org/10.1029/2018GL081475>.
- Rubel, F., Brugger, K., Haslinger, K. and Auer, I. (2017) The climate of the European Alps: shift of very high resolution Koppen-Geiger climate zones 1800-2100. *Meteorologische Zeitschrift*, 26(2), 115–125. <https://doi.org/10.1127/metz/2016/0816>.
- Rusticucci, M., Kyselý, J., Almeida, G. and Lhotka, O. (2016) Long-term variability of heat waves in Argentina and recurrence probability of the severe 2008 heat wave in Buenos Aires. *Theoretical and Applied Climatology*, 124(3–4), 679–689. <https://doi.org/10.1007/s00704-015-1445-7>.
- Saldías, G.S., Largier, J.L., Mendes, R., Pérez-Santos, I., Vargas, C. A. and Sobarzo, M. (2016) Satellite-measured interannual variability of turbid river plumes off Central-Southern Chile: spatial patterns and the influence of climate variability. *Progress in Oceanography*, 146, 212–222. <https://doi.org/10.1016/j.pocean.2016.07.007>.
- Sánchez, E., Solman, S., Remedio, A., Berbery, H., Samuelsson, P., Da Rocha, R., Mourão, C., Li, L., Marengo, J., De Castro, M. and Jacob, D. (2015) Regional climate modelling in claris-lpb: a concerted approach towards twentyfirst century projections of regional temperature and precipitation over south america. *Climate Dynamics*, 45(7), 2193–2212.
- Schumacher, V., Justino, F., Fernández, A., Meseguer-Ruiz, O., Sarricolea, P., Comin, A., Peroni Venancio, L. and Althoff, D. (2020) Comparison between observations and gridded data sets over complex terrain in the Chilean Andes: precipitation and temperature. *International Journal of Climatology*, 40(12), 5266–5288. <https://doi.org/10.1002/joc.6518>.
- Skamarock, W.C., Klemp, J.B., Duda, M.G., Fowler, L.D., Park, S.-H. and Ringler, T.D. (2012) A multiscale nonhydrostatic atmospheric model using centroidal voronoi tessellations and C-grid staggering. *Monthly Weather Review*, 140(9), 3090–3105. <https://doi.org/10.1175/MWR-D-11-00215.1>.
- Solman, S.A. (2013) Regional climate modeling over South America: a review. *Advances in Meteorology*, 2013, 504357. <https://doi.org/10.1155/2013/504357>.
- Solman, S.A. (2016) Systematic temperature and precipitation biases in the claris-lpb ensemble simulations over south america and possible implications for climate projections. *Climate Research*, 68(2–3), 117–136. <https://doi.org/10.3354/cr01362>.
- Solman, S.A. and Blázquez, J. (2019) Multiscale precipitation variability over South America: analysis of the added value of CORDEX RCM simulations. *Climate Dynamics*, 53(3–4), 1547–1565. <https://doi.org/10.1007/s00382-019-04689-1>.
- Solman, S.A., Sanchez, E., Samuelsson, P., da Rocha, R.P., Li, L., Marengo, J., Pessacg, N.L., Remedio, A.R.C., Chou, S.C., Berbery, H., Le Treut, H., de Castro, M. and Jacob, D. (2013) Evaluation of an ensemble of regional climate model simulations over south america driven by the era-interim reanalysis: model performance and uncertainties. *Climate Dynamics*, 41(5), 1139–1157. <https://doi.org/10.1007/s00382-013-1667-2>.
- Swain, D.L., Langenbrunner, B., Neelin, J.D. and Hall, A. (2018) Increasing precipitation volatility in twenty-first-century California. *Nature Climate Change*, 8(5), 427–433. <https://doi.org/10.1038/s41558-018-0140-y>.
- The NCAR Command Language (Version 6.6.2) (2020). Boulder, Colorado: UCAR/NCAR/CISL/TDD. Available at: <https://doi.org/10.5065/D6WD3XH5>.
- Ullrich, P.A. (2014). SquadGen: Spherical Quadrilateral Grid Generator. available online at <http://climate.ucdavis.edu/squadgen.php>.
- Undurraga, R., Vicuña, S. and Melo, O. (2020) Compensating water service interruptions to implement a safe-to-fail approach to climate change adaptation in urban water supply. *Water*, 12(6), 1540. <https://doi.org/10.3390/w12061540>.
- Valenzuela, R.A. and Garreaud, R.D. (2019) Extreme daily rainfall in central-southern Chile and its relationship with low-level horizontal water vapor fluxes. *Journal of Hydrometeorology*, 20(9), 1829–1850.
- van Kampenhout, L., Lenaerts, J.T.M., Lipscomb, W.H., Sacks, W. J., Lawrence, D.M., Slater, A.G. and van den Broeke, M.R. (2017) Improving the representation of polar snow and firn in the Community Earth System Model. *Journal of Advances in Modeling Earth Systems*, 9(7), 2583–2600. <https://doi.org/10.1002/2017MS000988>.
- van Kampenhout, L., Rhoades, A.M., Herrington, A.R., Zarzycki, C. M., Lenaerts, J.T.M., Sacks, W.J. and van den Broeke, M.R. (2019) Regional grid refinement in an earth system model: impacts on

- the simulated Greenland surface mass balance. *The Cryosphere*, 13, 1547–1564. <https://doi.org/10.5194/tc-13-1547-2019>.
- Viale, M., Valenzuela, R., Garreaud, R.D. and Ralph, F.M. (2018) Impacts of atmospheric rivers on precipitation in southern south america. *Journal of Hydrometeorology*, 19(10), 1671–1687. <https://doi.org/10.1175/JHM-D-18-0006.1>.
- Viviroli, D., Archer, D.R., Buytaert, W., Fowler, H.J., Greenwood, G.B., Hamlet, A.F., Huang, Y., Koboltschnig, G., Litaor, M.I., López-Moreno, J.I., Lorentz, S., Schädler, B., Schreier, H., Schwaiger, K., Vuille, M. and Woods, R. (2011) Climate change and mountain water resources: overview and recommendations for research, management and policy. *Hydrology and Earth System Sciences*, 15(2), 471–504. <https://doi.org/10.5194/hess-15-471-2011>.
- Vuille, M., Franquist, E., Garreaud, R., Lavado Casimiro, W.S. and Cáceres, B. (2015) Impact of the global warming hiatus on andean temperature. *Journal of Geophysical Research: Atmospheres*, 120(9), 3745–3757. <https://doi.org/10.1002/2015JD023126>.
- Wang, M. and Ullrich, P. (2018) Marine air penetration in california's central valley: meteorological drivers and the impact of climate change. *Journal of Applied Meteorology and Climatology*, 57(1), 137–154. <https://doi.org/10.1175/JAMC-D-17-0089.1>.
- Wang, M., Ullrich, P. and Millstein, D. (2018) The future of wind energy in California: future projections with the variable-resolution CESM. *Renewable Energy*, 127 (C), 242–257. <https://doi.org/10.1016/j.renene.2018.04>.
- Watterson, I.G., Bathols, J. and Heady, C. (2014) What influences the skill of climate models over the continents? *Bulletin of the American Meteorological Society*, 95(5), 689–700. <https://doi.org/10.1175/BAMS-D-12-00136.1>.
- Wehner, M.F., Reed, K.A., Li, F., Prabhat, J.B., Chen, C.-T., Paciorek, C., Gleckler, P.J., Sperber, K.R., Collins, W.D., Gettelman, A. and Jablonowski, C. (2014) The effect of horizontal resolution on simulation quality in the Community Atmospheric Model, CAM5.1. *Journal of Advances in Modeling Earth Systems*, 6(4), 980–997. <https://doi.org/10.1002/2013MS000276>.
- Wilks, D.S. (2016) “The stippling shows statistically significant grid points”: how research results are routinely overstated and Over-interpreted, and what to do about it. *Bulletin of the American Meteorological Society*, 97(12), 2263–2273. <https://doi.org/10.1175/BAMS-D-15-00267.1>.
- Willmott, C.J. and Matsuura, K. (1995) Smart interpolation of annually averaged air temperature in the United States. *Journal of Applied Meteorology*, 34(12), 2577–2586. [https://doi.org/10.1175/1520-0450\(1995\)034<2577:SIOAAA>2.0.CO;2](https://doi.org/10.1175/1520-0450(1995)034<2577:SIOAAA>2.0.CO;2).
- Willmott, C.J. and Robeson, S.M. (1995) Climatologically aided interpolation (CAI) of terrestrial air temperature. *International Journal of Climatology*, 15(2), 221–229. <https://doi.org/10.1002/joc.3370150207>.
- Woelfle, M.D., Bretherton, C.S., Hannay, C. and Neale, R. (2019) Evolution of the double-ITCZ bias through cesm2 development. *Journal of Advances in Modeling Earth Systems*, 11(7), 1873–1893. <https://doi.org/10.1029/2019MS001647>.
- Wu, C., Liu, X., Lin, Z., Rhoades, A.M., Ullrich, P.A., Zarzycki, C. M., Lu, Z. and Rahimi-Esfarjani, S.R. (2017) Exploring a variable-resolution approach for simulating regional climate in the rocky mountain region using the vr-cesm. *Journal of Geophysical Research: Atmospheres*, 122(20), 10939–10965. <https://doi.org/10.1002/2017JD027008>.
- Xu, Z., Rhoades, A.M., Johansen, H., Ullrich, P.A. and Collins, W.D. (2018) An intercomparison of gcm and rcm dynamical downscaling for characterizing the hydroclimatology of California and Nevada. *Journal of Hydrometeorology*, 19(9), 1485–1506.
- Zarzycki, C.M. (2016) Tropical cyclone intensity errors associated with lack of two-way ocean coupling in high-resolution global simulations. *Journal of Climate*, 29, 8589–8610. <https://doi.org/10.1175/JCLI-D-16-0273.1>.
- Zarzycki, C.M. and Jablonowski, C. (2014) A multidecadal simulation of Atlantic tropical cyclones using a variable-resolution global atmospheric general circulation model. *Journal of Advances in Modeling Earth Systems*, 6(3), 805–828. <https://doi.org/10.1002/2014MS000352>.
- Zarzycki, C.M., Jablonowski, C. and Taylor, M.A. (2014a) Using variable resolution meshes to model tropical cyclones in the community atmosphere model. *Monthly Weather Review*, 142(3), 1221–1239. <https://doi.org/10.1175/MWR-D-13-00179.1>.
- Zarzycki, C.M., Jablonowski, C., Thatcher, D.R. and Taylor, M.A. (2015) Effects of localized grid refinement on the general circulation and climatology in the community atmosphere model. *Journal of Climate*, 28(7), 2777–2803. <https://doi.org/10.1175/JCLI-D-14-00599.1>.
- Zarzycki, C.M., Levy, M.N., Jablonowski, C., Overfelt, J.R., Taylor, M. A. and Ullrich, P.A. (2014b) Aquaplanet experiments using CAM's variable-resolution dynamical Core. *Journal of Climate*, 27, 5481–5503. <https://doi.org/10.1175/JCLI-D-14-00004.1>.
- Zarzycki, C.M., Reed, K.A., Bacmeister, J.T., Craig, A.P., Bates, S.C. and Rosenbloom, N.A. (2016) Impact of surface coupling grids on tropical cyclone extremes in high-resolution atmospheric simulations. *Geoscientific Model Development*, 9(2), 779–788. <https://doi.org/10.5194/gmd-9-779-2016>.

SUPPORTING INFORMATION

Additional supporting information may be found in the online version of the article at the publisher's website.

How to cite this article: Bambach, N. E., Rhoades, A. M., Hatchett, B. J., Jones, A. D., Ullrich, P. A., & Zarzycki, C. M. (2021). Projecting climate change in South America using variable-resolution Community Earth System Model: An application to Chile. *International Journal of Climatology*, 1–29. <https://doi.org/10.1002/joc.7379>